Study of Single W & $WW\gamma$ Couplings

Haijun Yang

June 4, 1999

Contents :

- Introduction of TGCs
- Data & Monte Carlo
- Single W Definition
- Events Selection
- Measurement of Cross Section
- Anomalous Couplings Fit
- Conclusions
- Acknowledgements

CERN

Introduction of TGCs

Triple-Gauge-Boson self-Couplings (TGCs) are the most direct consequence of the non-Abelian $SU(2) \times U(1)$ gauge theory. The couplings are uniquely determined by the Standard Model (SM). Any deviation of these couplings from SM predictions would indicate New Physics (NP).

There are 5 (CP) + 1 (CP, $\bar{C}$ & $\bar{P}$) + 3 ($\overline{CP}$) = 9 independent couplings . A complete list of independent couplings shows in Table 1.

Effective Lagrangian splits into 3 pieces:

$$\begin{aligned} L = \quad & L_1(C \textit{ and } P \textit{ conserving}) + \\ & L_2(CP \textit{ conserving}, \ C \ \& \ P \textit{ violating}) + \\ & L_3(CP \textit{ violating}) \end{aligned}$$

CERN

Introduction of TGCs

Table 1: Complete list of the possible TGCs.

	CP Conserving		CP Violating
	$W^+W^-\gamma$	$W^+W^-Z^0$	$W^+W^-Z^0$
charge	e	g_{WWZ}	
magnetic dipole (μ_W)	κ_γ	κ_Z	$\hat{\kappa}_Z(\bar{P}),\ \hat{\hat{\kappa}}_Z(\bar{C})$
electric quadrupole (Q_W)	λ_γ	λ_Z	$\hat{\lambda}_Z$
anapole		$z_Z(\bar{C},\ \bar{P})$	

$$\mu_W = \frac{e}{2M_W}(1+\kappa_\gamma+\lambda_\gamma)$$

$$Q_W = -\frac{e}{M_W^2}(\kappa_\gamma-\lambda_\gamma)$$

Introduction of TGCs

Effective Lagrangian:

$$
\begin{aligned}
L_1 = \quad & -ie[A_\mu(W^{-\mu\nu}W^+_\nu - W^{+\mu\nu}W^-_\nu) \\
& +\kappa_\gamma F_{\mu\nu}W^{+\mu}W^{-\nu}] \\
& -ieg_{ZWW}[Z_\mu(W^{-\mu\nu}W^+_\nu - W^{+\mu\nu}W^-_\nu) \\
& +\kappa_Z Z_{\mu\nu}W^{+\mu}W^{-\nu}] \\
& +ie\frac{\lambda_\gamma}{M_W^2}F^{\nu\lambda}W^-_{\lambda\mu}W^{+\mu}_\nu \\
& +iectg\theta_W\frac{\lambda_Z}{M_W^2}Z^{\nu\lambda}W^-_{\lambda\mu}W^{+\mu}_\nu
\end{aligned}
\tag{1}
$$

$$
\begin{aligned}
L_2 = \quad & \frac{ez_Z}{M_W^2}\partial_\alpha\hat{Z}_{\rho\sigma}(\partial^\rho W^{-\sigma}W^{+\alpha} - \partial^\rho W^{-\alpha}W^{+\sigma} \\
& +\partial^\rho W^{+\sigma}W^{-\alpha} - \partial^\rho W^{+\alpha}W^{-\sigma})
\end{aligned}
\tag{2}
$$

$$
\begin{aligned}
L_3 = \quad & iectg\theta_W[\hat{\kappa}_Z\hat{Z}_{\mu\nu}W^{+\mu}W^{-\nu} \\
& +\frac{\hat{\lambda}_Z}{M_W^2}\hat{Z}^{\nu\lambda}W^+_{\lambda\mu}W^{-\mu}_\nu] \\
& +ectg\theta_W\hat{\hat{\kappa}}_Z(\partial^\mu Z^\nu + \partial^\nu Z^\mu)W^+_\mu W^-_\nu
\end{aligned}
\tag{3}
$$

CERN

Introduction of TGCs

where

$$\begin{cases} W^{\pm}_{\mu\nu} \equiv \partial_\mu W^{\pm}_\nu - \partial_\nu W^{\pm}_\mu \\ Z_{\mu\nu} \equiv \partial_\mu Z_\nu - \partial_\nu Z_\mu \\ \hat{Z}_{\rho\sigma} \equiv \frac{1}{2}\epsilon_{\rho\sigma\alpha\beta} Z^{\alpha\beta} \end{cases} \tag{4}$$

For practical purposes, it's convenient to introduce deviations from the SM predictions:

$$\begin{cases} \Delta g_1^Z \equiv g_1^Z - 1 \\ \Delta\kappa_\gamma \equiv \kappa_\gamma - 1 \\ \Delta\kappa_Z \equiv \kappa_Z - 1 \\ \lambda_\gamma \ , \quad \lambda_Z \end{cases} \tag{5}$$

Considering the $SU(2) \times U(1)$ gauge theory can be realized linearly, only 3 of 5 couplings are independent:

$$\begin{cases} \Delta\kappa_\gamma = -cot^2\theta_W(\Delta\kappa_Z - \Delta g_1^Z) \\ \lambda_\gamma = \lambda_Z \end{cases} \tag{6}$$

CERN

Introduction of TGCs

- Hadron Collider(p^+p^-): At Fermilab, TGCs have been studied by CDF and DØ, using

$$\left\{\begin{array}{l} p^+p^- \rightarrow W\gamma \rightarrow e\nu_e\gamma,\ \mu\nu_\mu\gamma \\ p^+p^- \rightarrow WW \rightarrow l\nu_l qq \\ p^+p^- \rightarrow WW/WZ \rightarrow l\nu_l qq,\ l^+l^-qq. \end{array}\right.$$

- e^+e^- Collider: At LEP2, TGCs have been directly measured by four Experiments, ALEPH, DELPHI, L3 and OPAL, using

$$\left\{\begin{array}{l} e^+e^- \rightarrow W^+W^- \rightarrow l\nu_l qq,\ qqqq \\ e^+e^- \rightarrow e^+\nu_e W^- \rightarrow e^+\nu_e l^-\bar{\nu}_l,\ e^+\nu_e q\bar{q}' \\ e^+e^- \rightarrow \nu\bar{\nu}\gamma. \end{array}\right.$$

CERN

Introduction of TGCs

$e^+e^- \rightarrow W^+W^-$ Production

- Advantage: high sensitivity to $WW\gamma$ and WWZ couplings.
- Disadvantage: cannot separate $WW\gamma$ and WWZ.

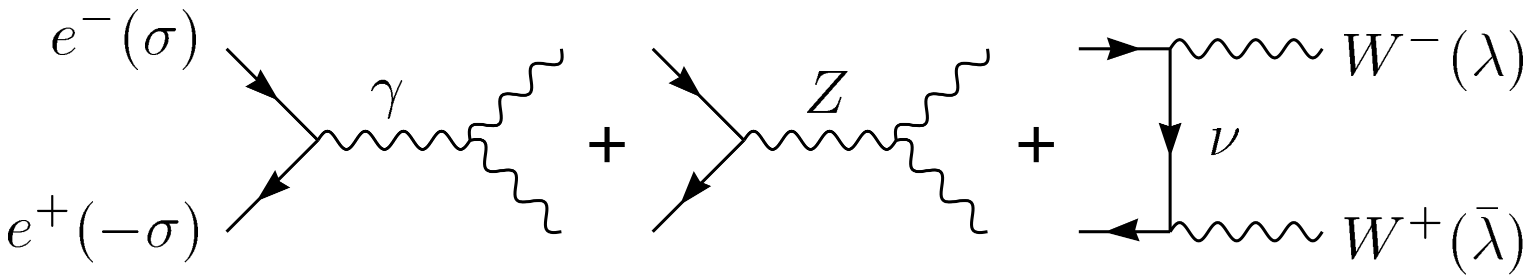

Figure 1: $e^+e^- \rightarrow W^+W^-$ Feynman diagrams.

Introduction of TGCs

$e^+e^- \rightarrow \nu\bar{\nu}\gamma$ Production

- Advantage: only sensitive to $WW\gamma$ vertex.
- Disadvantage: low sensitivity to $WW\gamma$.

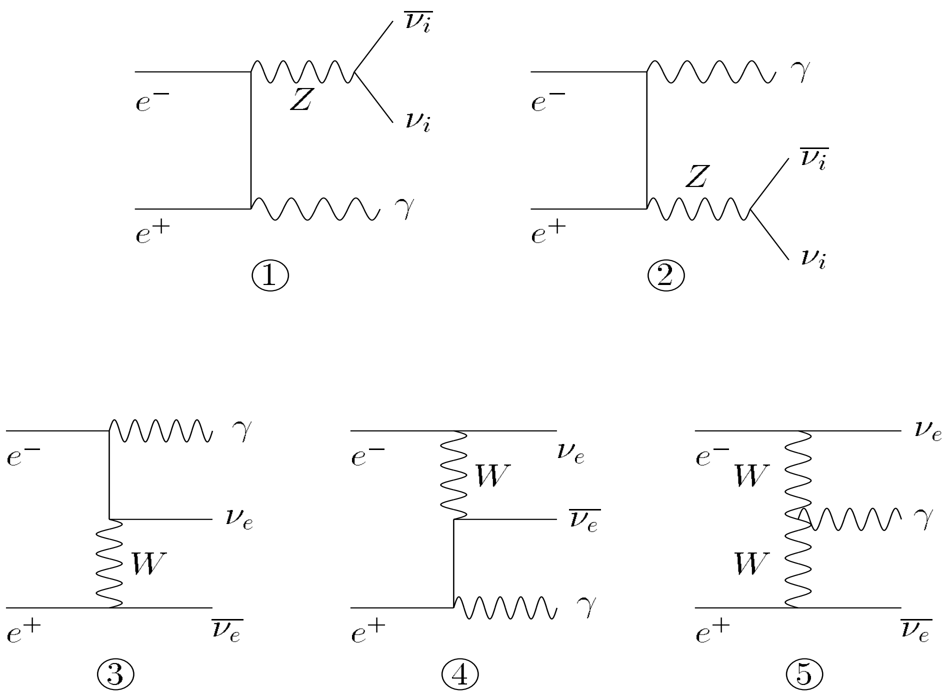

Figure 2: $e^+e^- \rightarrow \nu\bar{\nu}\gamma$ Feynman diagrams.

CERN

Introduction of TGCs

$e^+e^- \to e^+\nu_e W^-$ Production

- Advantage: only sensitive to $WW\gamma$, $\Delta\kappa_\gamma$ is comparable to that from W pairs.
- Disadvantage: λ_γ is not so attractive.

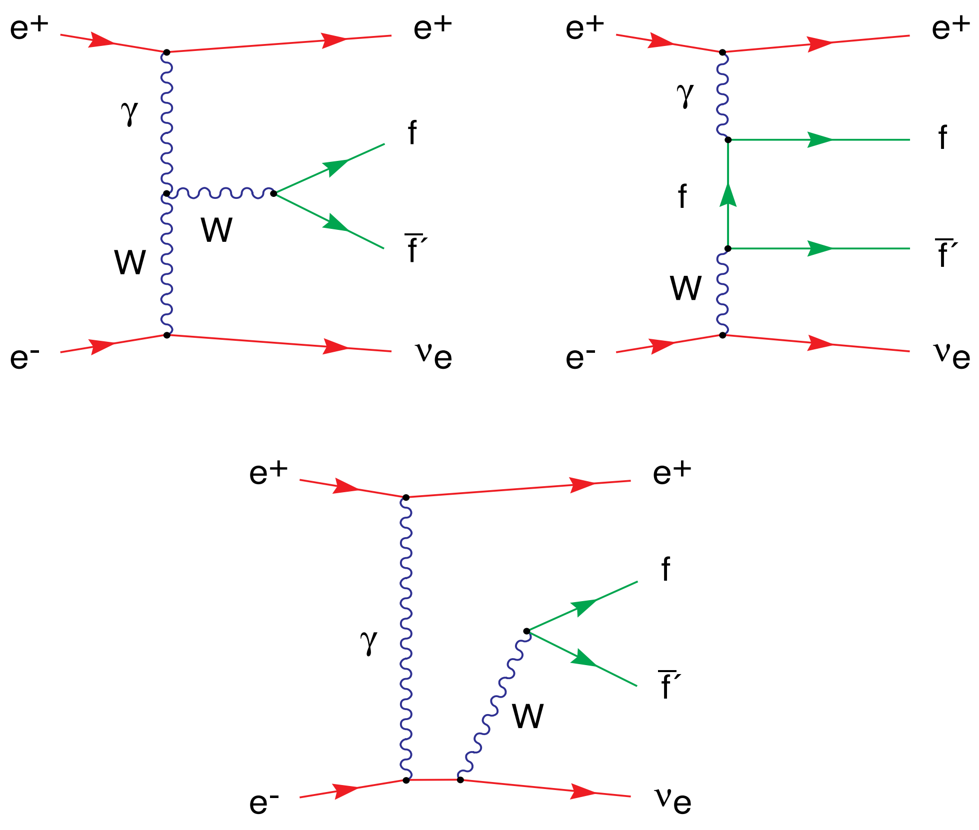

Figure 3: $e^+e^- \to e^+\nu_e W^-$ Feynman diagrams.

Introduction of TGCs

The cross section of Single W production is only dependent on $\Delta\kappa_\gamma$ and λ_γ.

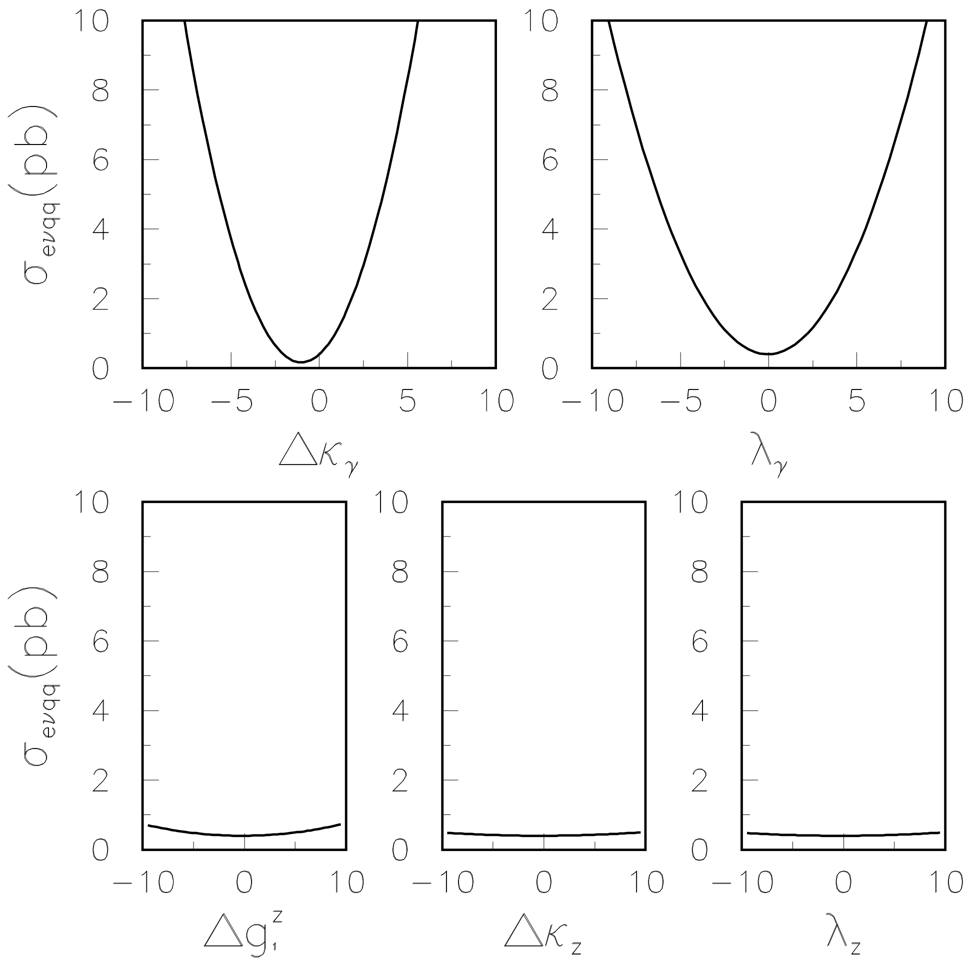

Figure 4: Cross section of $e^+\nu_e W^- \to e^+\nu_e q\bar{q}'$ as a function of A.C. at $\sqrt{s} = 189\ GeV$.

CERN

Data & Monte Carlo

Data sample was collected by L3 detector at $\sqrt{s} = 189\ GeV$ in 1998. Total integrated luminosity $\mathcal{L} = 176.4\ pb^{-1}$.

Monte Carlo (Events Generator):

- Single W hadronic final states:
  Signal: $e^+\nu_e l^- \bar{\nu}_l$
  Background:
  EXCALIBUR: $e^+\nu_e l^- \bar{\nu}_l$, $l^+\nu_l l^- \bar{\nu}_l$, $llll$
  TEEGG: $e^+e^-(\gamma)$
  KORALZ: $\mu^+\mu^-$, $\tau^+\tau^-$, $\nu\bar{\nu}(\gamma)$
- Single W leptonic final states:
  Signal: $e^+\nu_e q\bar{q}'$
  Background:
  KORALW: W^+W^-
  PYTHIA: Z^0Z^0, $q\bar{q}$, $Z^0e^+e^-$
  PHOJET: $e^+e^-q\bar{q}$

Single W Definition

The signal is defined as $e^+e^- \rightarrow e^+\nu_e f\bar{f}'$ events that satisfy the following phase space cuts:

$$\begin{aligned} |cos\theta_{e^+}| &> 0.997 \\ min(E_f, E_{\bar{f}'}) &> 15\ GeV \\ |cos\theta_{e^-}| &< 0.75,\ e^+\nu_e e^-\bar{\nu}_e\ only \end{aligned} \tag{7}$$

Table 2: Evaluation of non-resonant final states after Single W definition, $\Delta M = |M_{f\bar{f}'} - M_W|$.

channels	$\Delta M > 15GeV$	$\Delta M > 20GeV$
$W^- \rightarrow e^-\bar{\nu}_e$	22.9%	18.4%
$W^- \rightarrow \mu^-\bar{\nu}_\mu$	11.5%	9.6%
$W^- \rightarrow \tau^-\bar{\nu}_\tau$	12.5%	9.2%
$W^- \rightarrow q\bar{q}'$	9.6%	7.6%
Total	11.6%	9.2%

CERN

Single W Definition

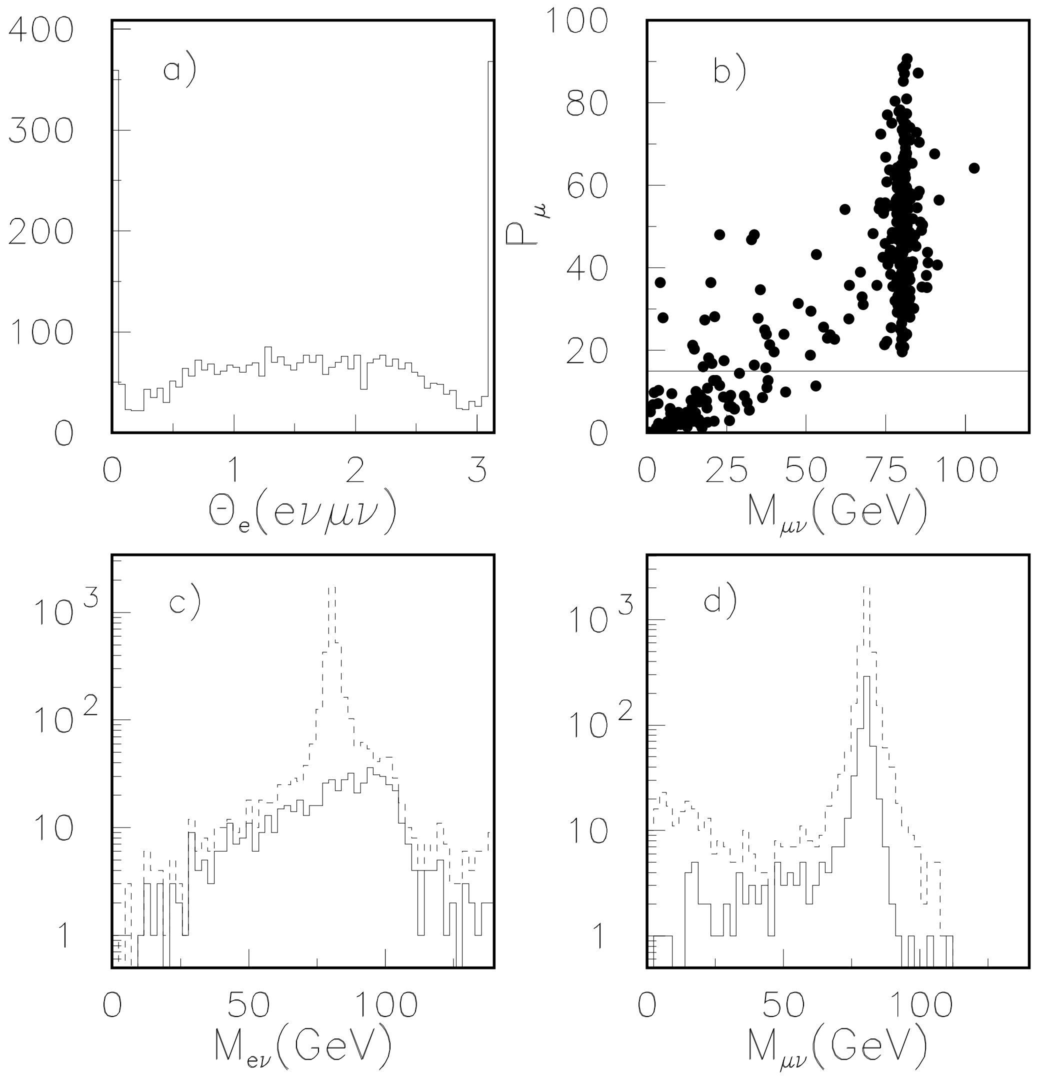

Figure 5: $e^+e^- \to e^+\nu_e\mu^-\bar{\nu}_\mu$.

CERN

Single W Definition

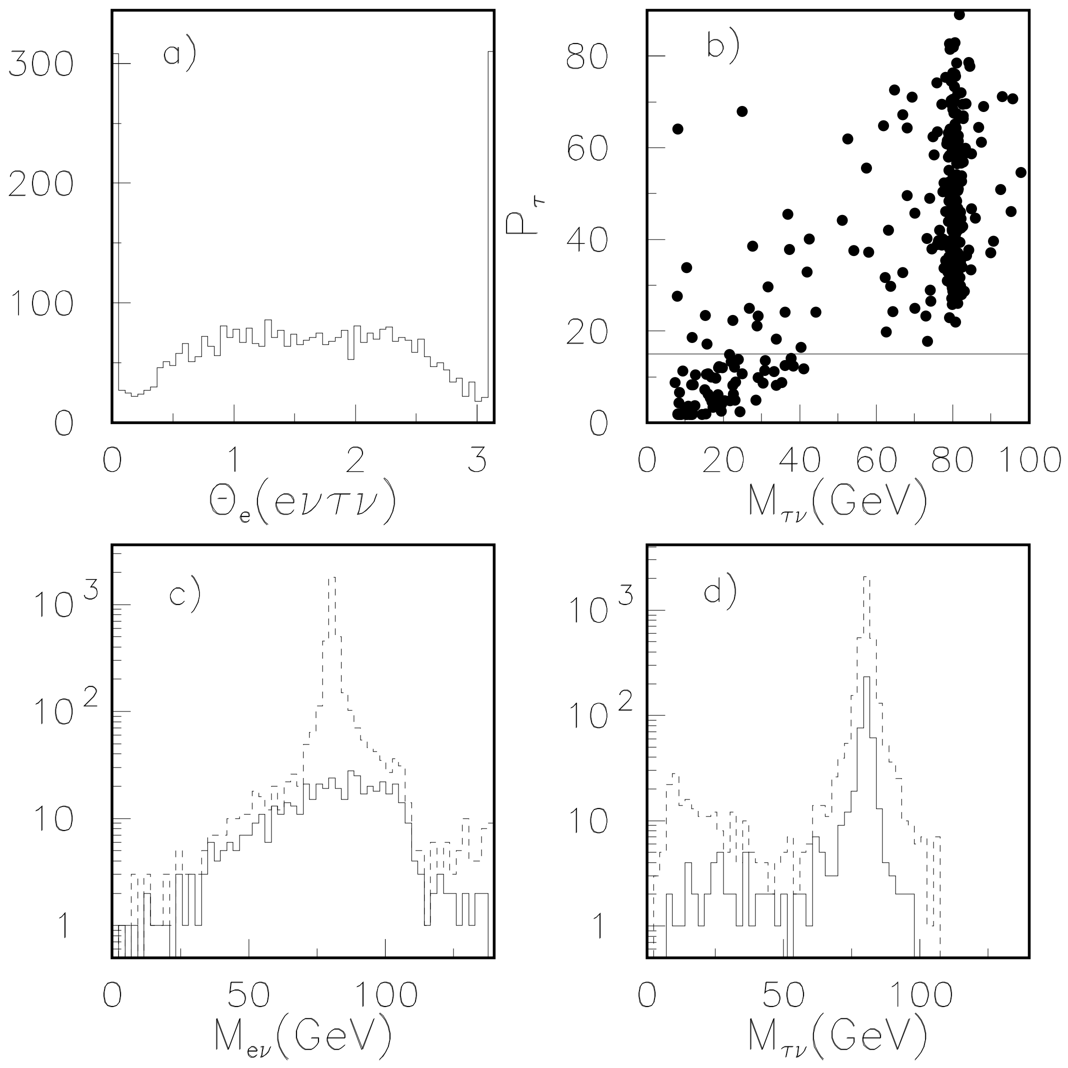

Figure 6: $e^+e^- \rightarrow e^+\nu_e\tau^-\bar{\nu}_\tau$.

Single W Definition

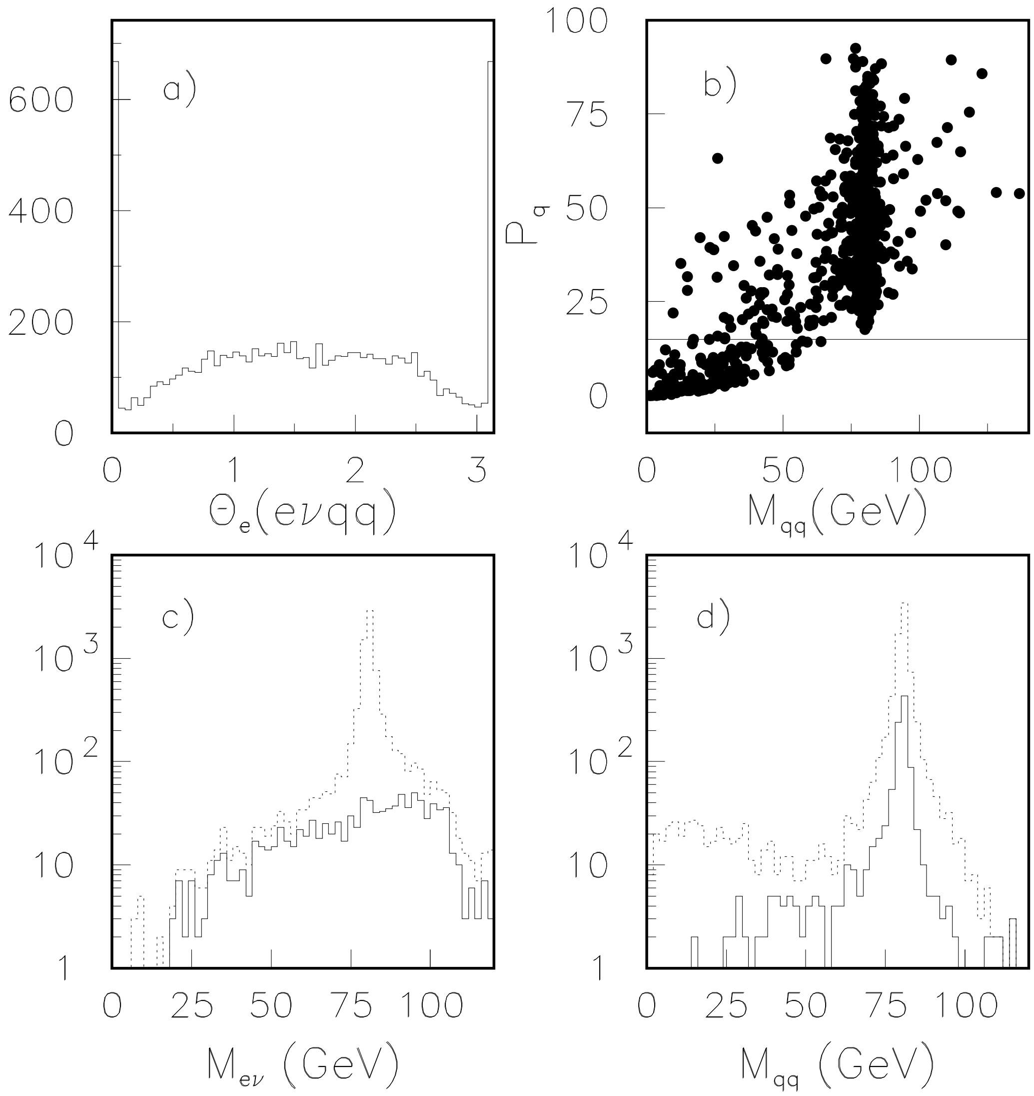

Figure 7: $e^+e^- \to e^+\nu_e q\bar{q}'$.

Events Selection

Single W leptonic final states, $W^- \to l^- \bar{\nu}_l$.
Good TEC track definition:

- $N_{hits} > 20$
- $SPAN > 30$
- $|DCA| < 5\ mm$
- $P_t > 100\ MeV$

Single W hadronic final states, $W^- \to q\bar{q}'$.
Good TEC track definition:

- $N_{hits} > 20$
- $SPAN > 30$
- $|DCA| < 10\ mm$
- $P_t > 100\ MeV$

CERN

Events Selection

Selection cuts for $W^- \rightarrow e^-\bar{\nu}_e$:

(1) $N_{trk} = 1$

(2) $|cos(\theta_{trk})| < 0.7$

(3) $\theta_{trk-bump} < 10^\circ$

(4) $E_{bump} > 20\ GeV$

(5) $E_{bump}/E_{tot} > 0.93$

(6) $E_{cone>15^\circ} < 3\ GeV$

(7) $E_{lumi} + E_{alr} < 65 GeV$

Main backgrounds after selection:
$e^+e^-\nu_l\bar{\nu}_l$, $e^+\nu_e\mu^-\bar{\nu}_\mu$, $e^+\nu_e\tau^-\bar{\nu}_\tau$, $e^+e^-(\gamma)$, $\nu\bar{\nu}(\gamma)$.

CERN

Events Selection

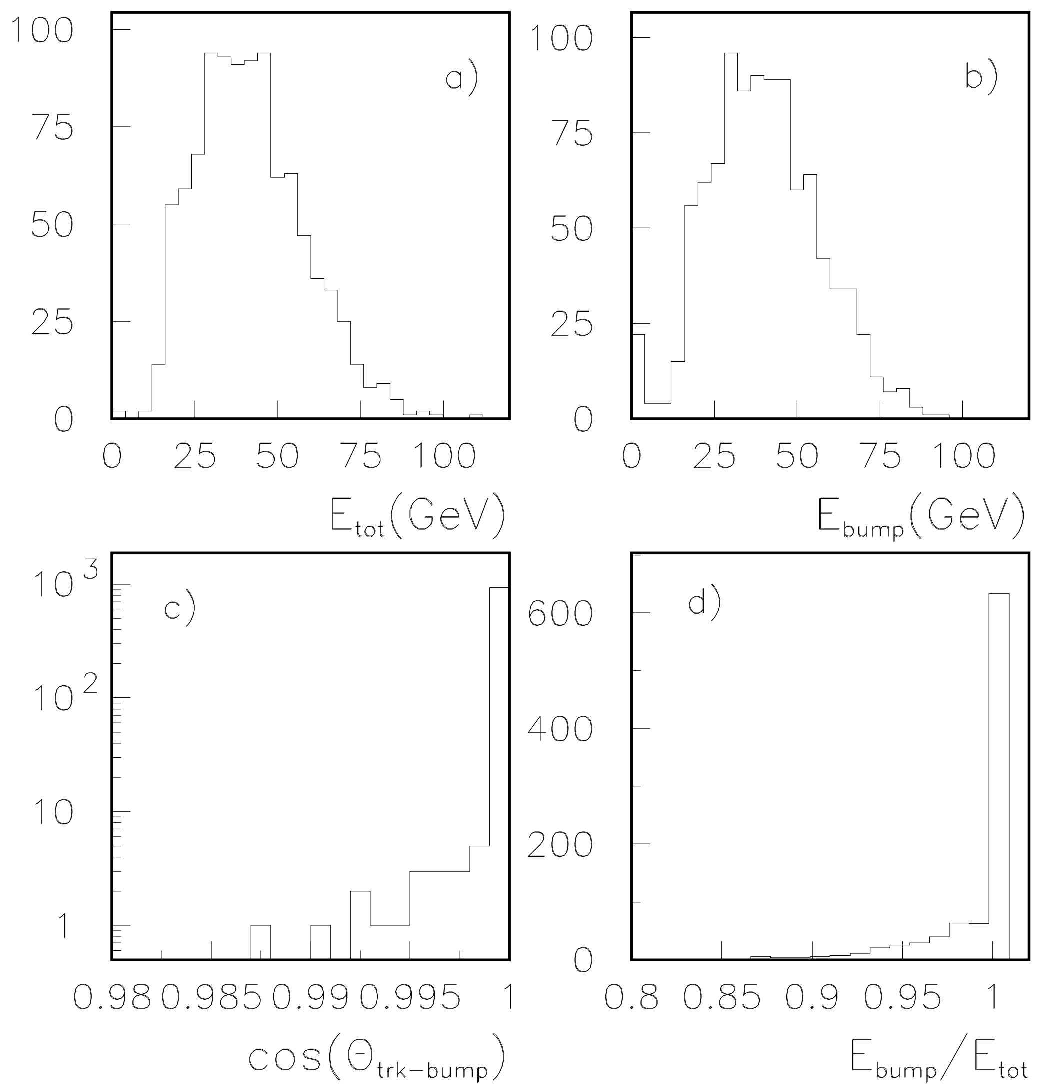

Figure 8: $W^- \to e^- \bar{\nu}_e$

CERN

Events Selection

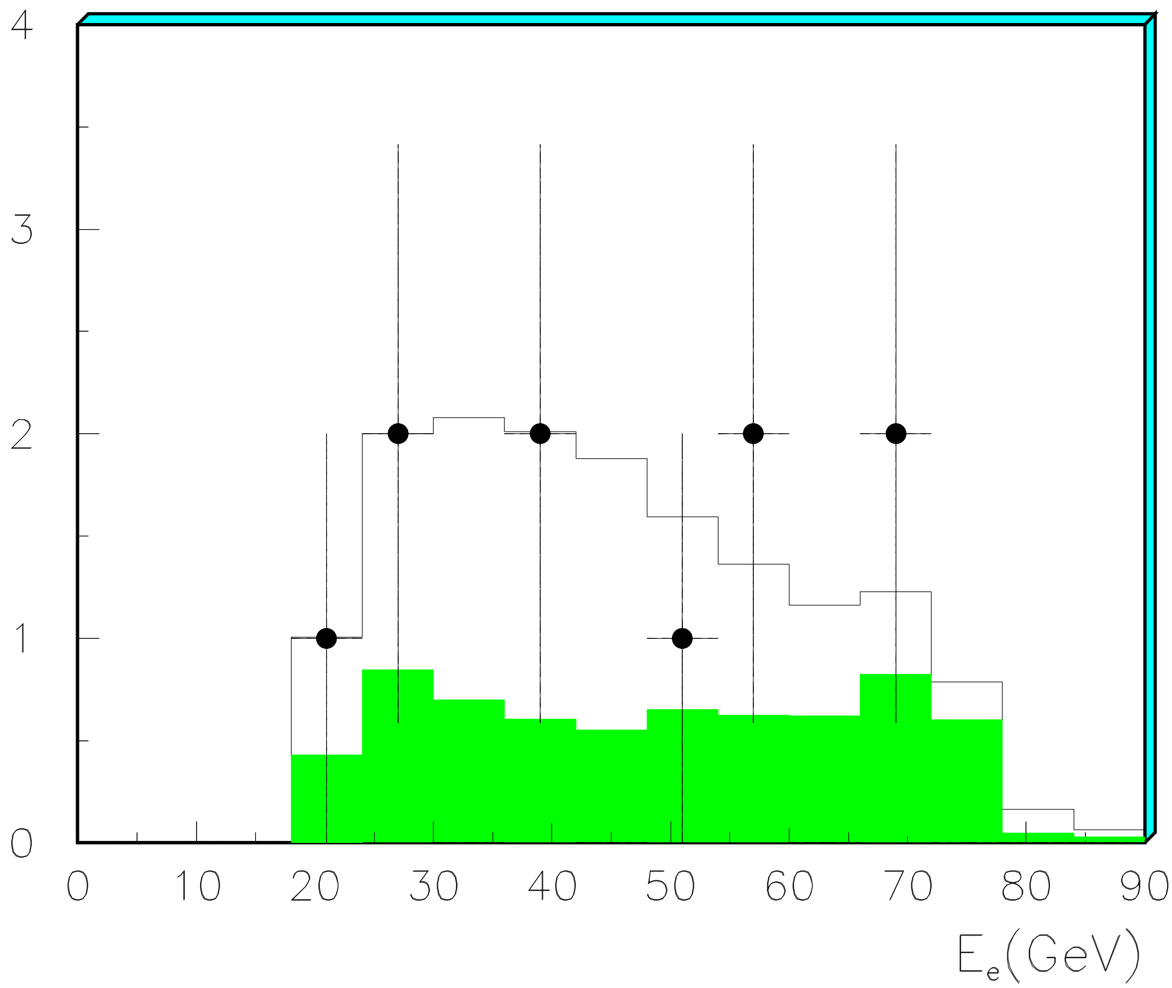

Figure 9: $W^- \to e^-\bar{\nu}_e$

Channel	Signal	BG	(Data)	Eff.(%)
$W^- \to e^-\bar{\nu}_e$	8.8	6.2	10	81.5

CERN

Events Selection

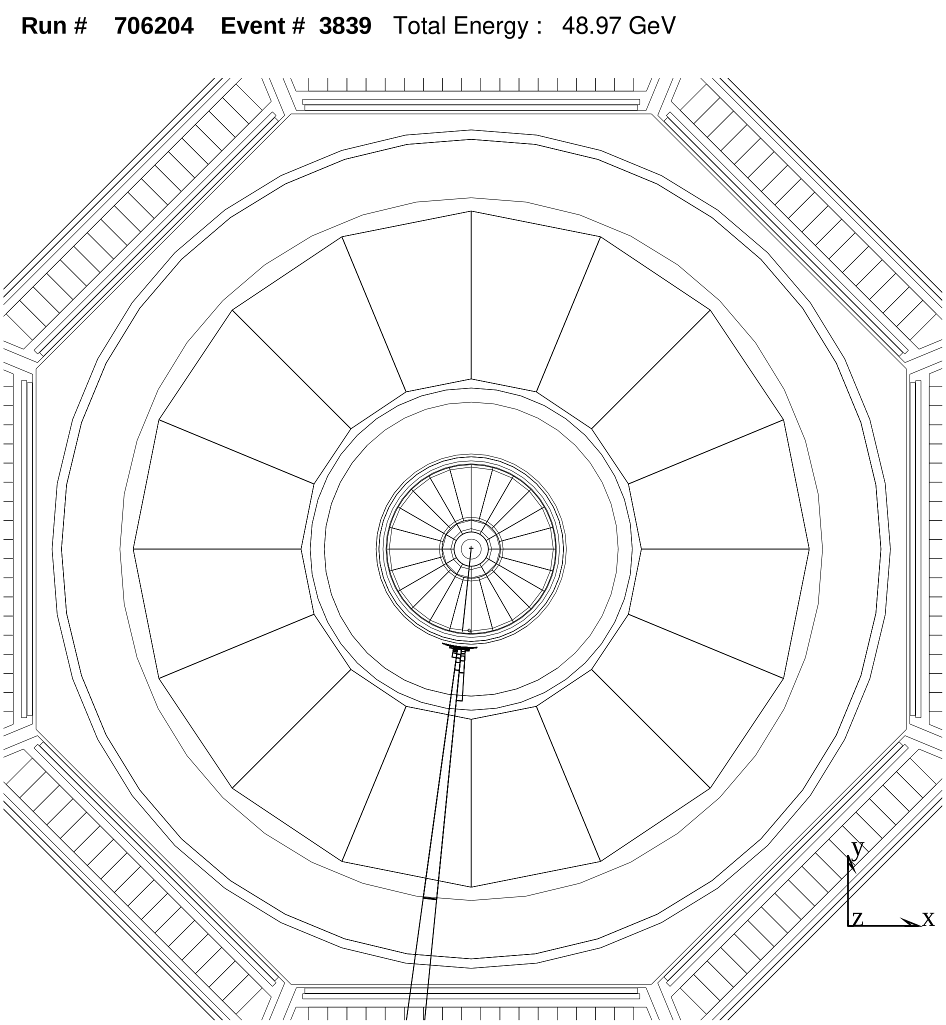

Figure 10: $W^- \rightarrow e^- \bar{\nu}_e$ candidate

$N_{trk} = 1, \quad N_{hits} = 58, \quad SPAN = 62,$
$E_{bgo} = 48.4\ GeV, \quad E_{tot} = 49 GeV.$

Events Selection

Selection cuts for $W^- \to \mu^- \bar{\nu}_\mu$:

(1) $N_{trk} = 1$

(2) $\theta_{trk-\mu} < 10^\circ$

(3) $P_\mu = E_\mu > 20\ GeV$

(4) $E_\mu / E_{tot} > 0.93$

(5) $E_{bgo} < 0.6\ GeV$

(6) $E_{hcal} < 8\ GeV$

(7) $|TOF| < 5\ ns$

(8) $E_{lumi} + E_{alr} < 65 GeV$

Main backgrounds after selection:
$\mu^+\mu^-$, $e^+\nu_e\mu^-\bar{\nu}_\mu$, $\mu^+\nu_\mu\mu^-\bar{\nu}_\mu$, $\mu^+\nu_\mu\tau^-\bar{\nu}_\tau$.

CERN

Events Selection

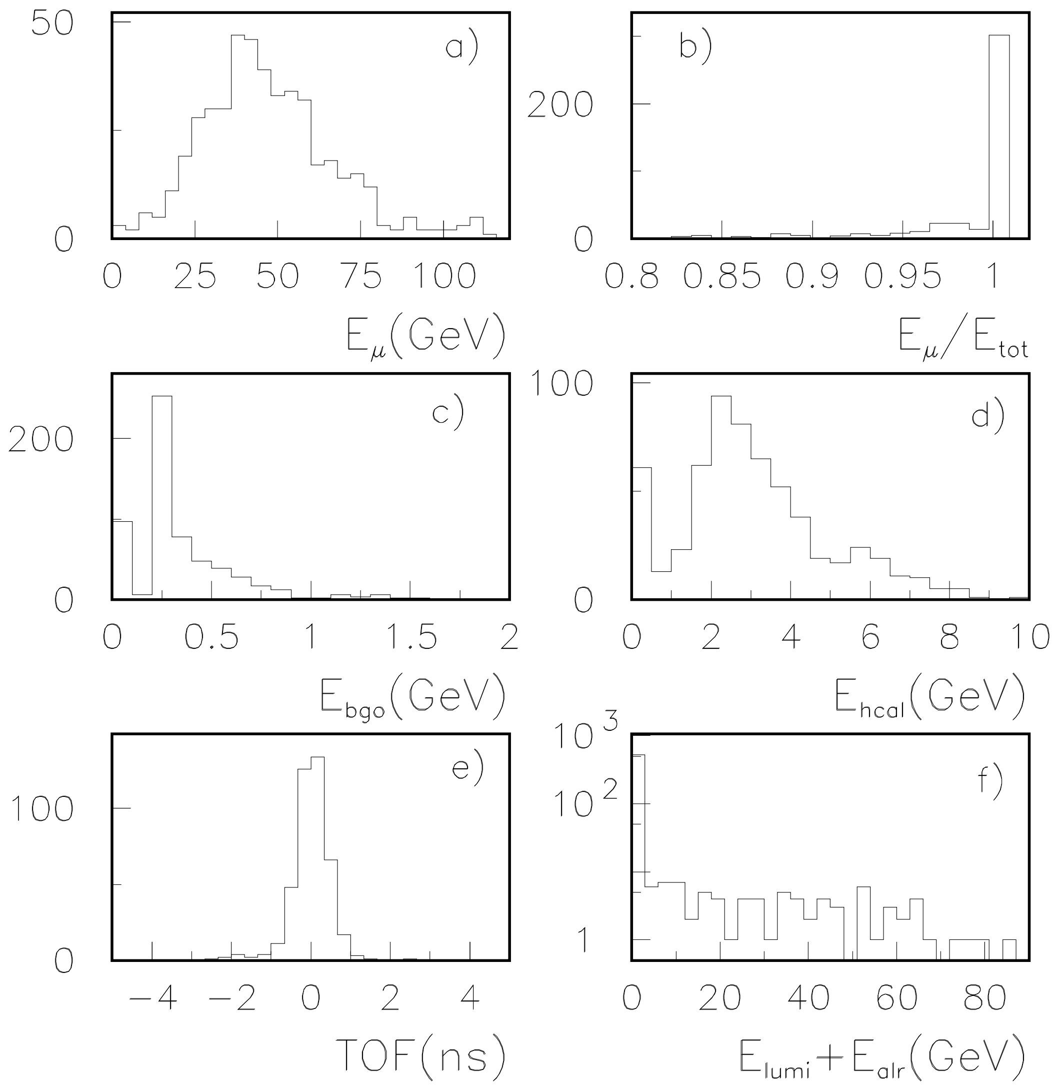

Figure 11: $W^- \rightarrow \mu^- \bar{\nu_\mu}$

CERN

Events Selection

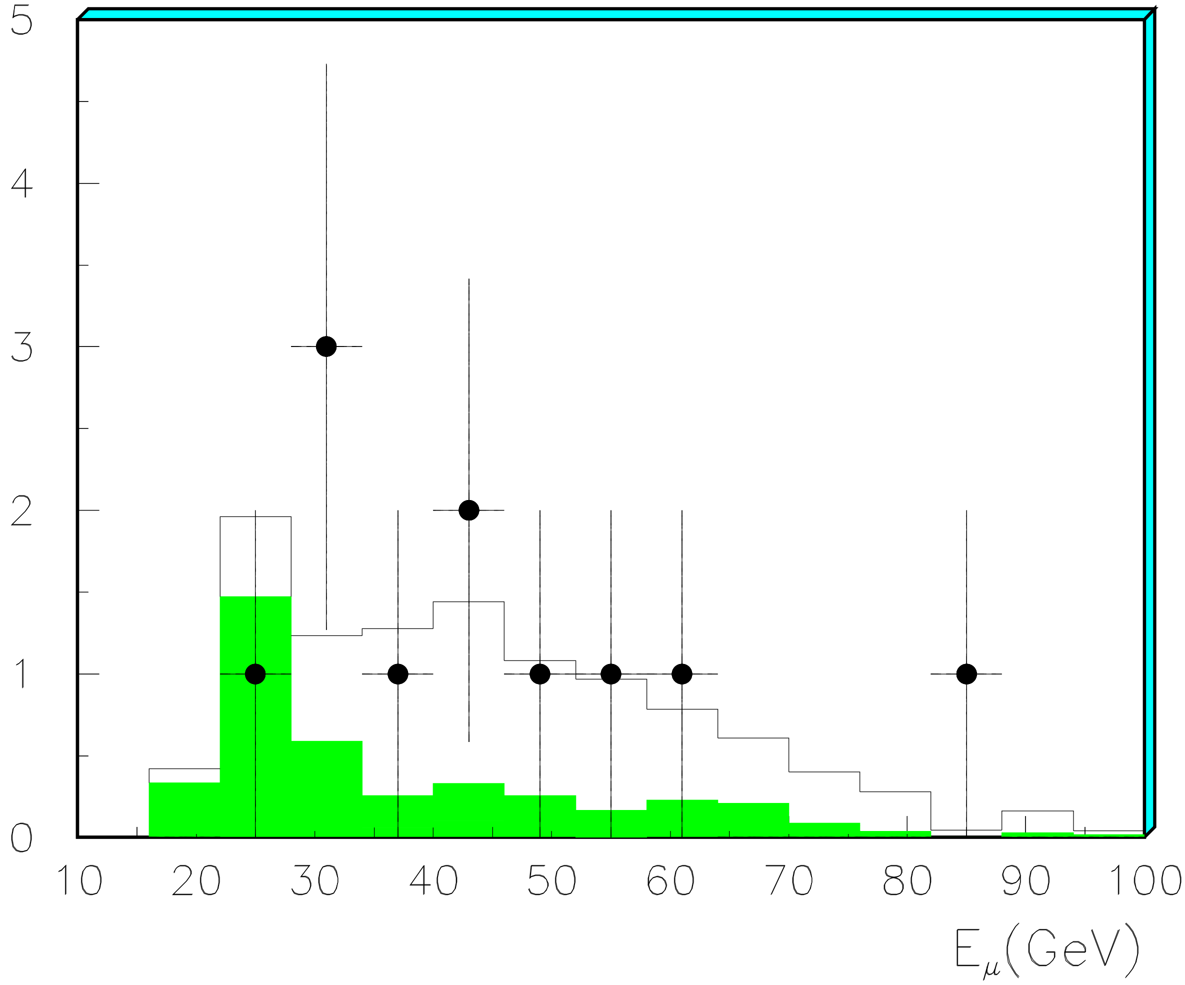

Figure 12: $W^- \to \mu^- \bar{\nu}_\mu$

Channel	Signal	BG	(Data)	Eff.(%)
$W^- \to \mu^- \bar{\nu}_\mu$	6.7	4.0	13	51.1

CERN

Events Selection

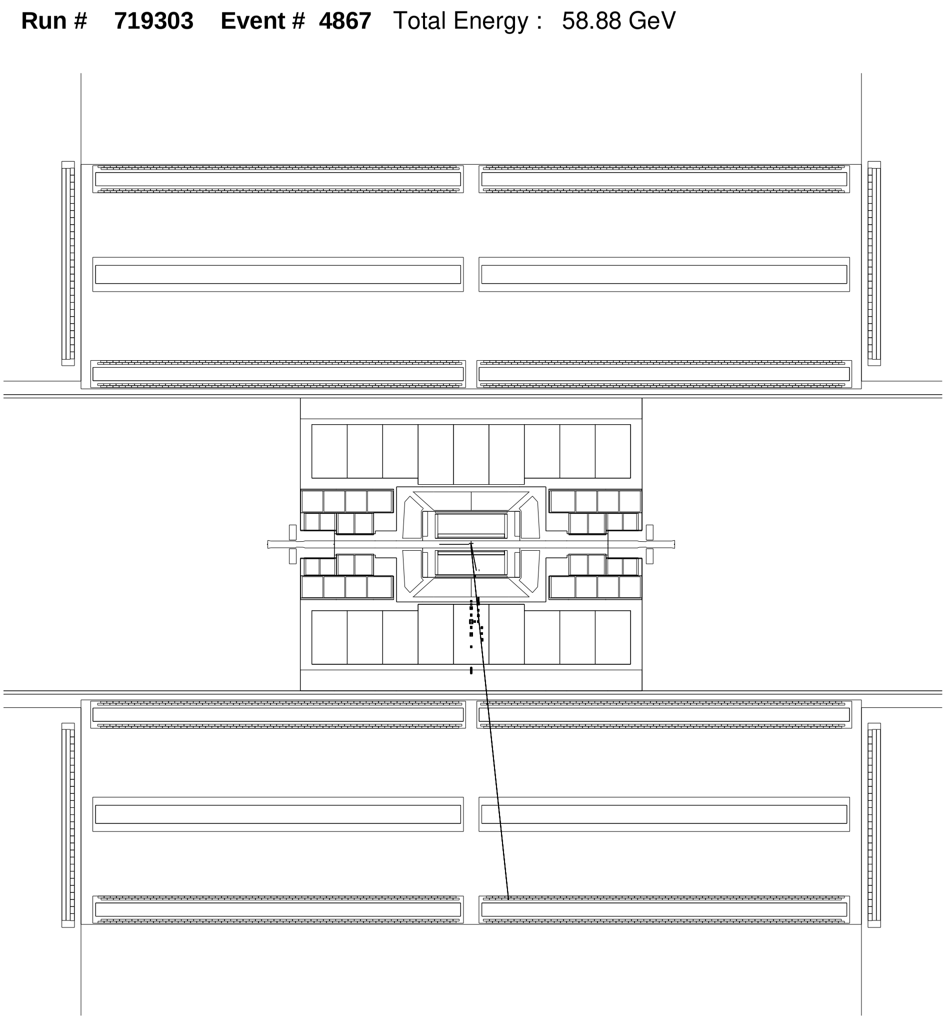

Figure 13: $W^- \rightarrow \mu^- \bar{\nu_\mu}$ candidate

$N_{trk} = 1,\ \theta_{trk-\mu} = 4.2^\circ, E_{bgo} = 0.24\ GeV,$
$E_{hcal} = 2.47\ GeV,\ E_\mu = 58.6\ GeV.$

CERN

Events Selection

Selection cuts for $W^- \to \tau^- \bar{\nu_\tau}$:

(1) $N_{trk} = 1 \ or \ 3$

(2) $N_{sjt} = 1$

(3) $|cos(\theta_{sjt})| < 0.74$

(4) $E_{sjt} > 15 \ GeV$

(5) $E_{bgo}/E_{tot} < 0.85$

(6) $E_{lumi} + E_{alr} < 65 GeV$

Main backgrounds after selection:
$\tau^+\tau^-$, $e^+\nu_e\tau^-\bar{\nu_\tau}$, $\mu^+\nu_\mu\tau^-\bar{\nu_\tau}$, $\tau^+\nu_\tau\tau^-\bar{\nu_\tau}$.

CERN

Events Selection

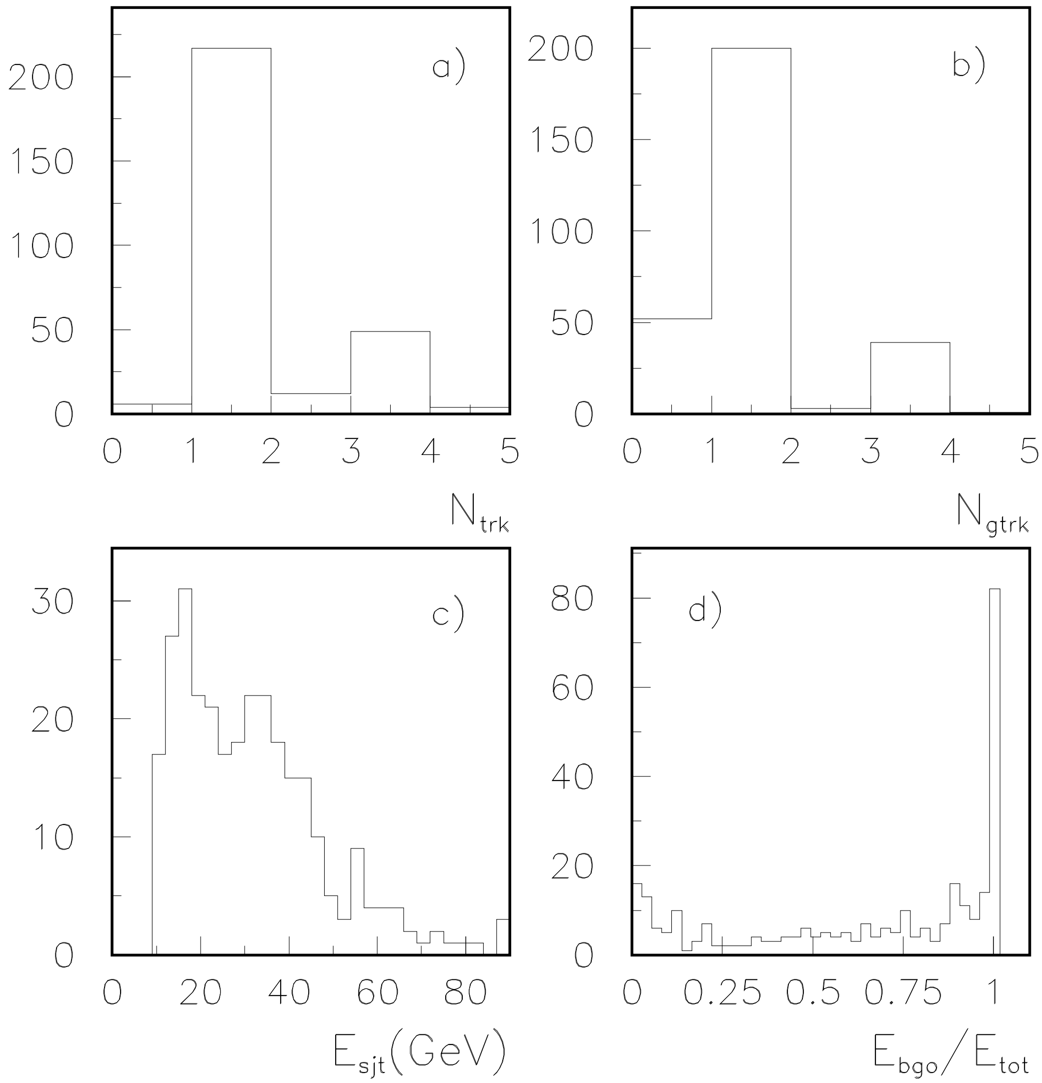

Figure 14: $W^- \to \tau^- \bar{\nu_\tau}$

Events Selection

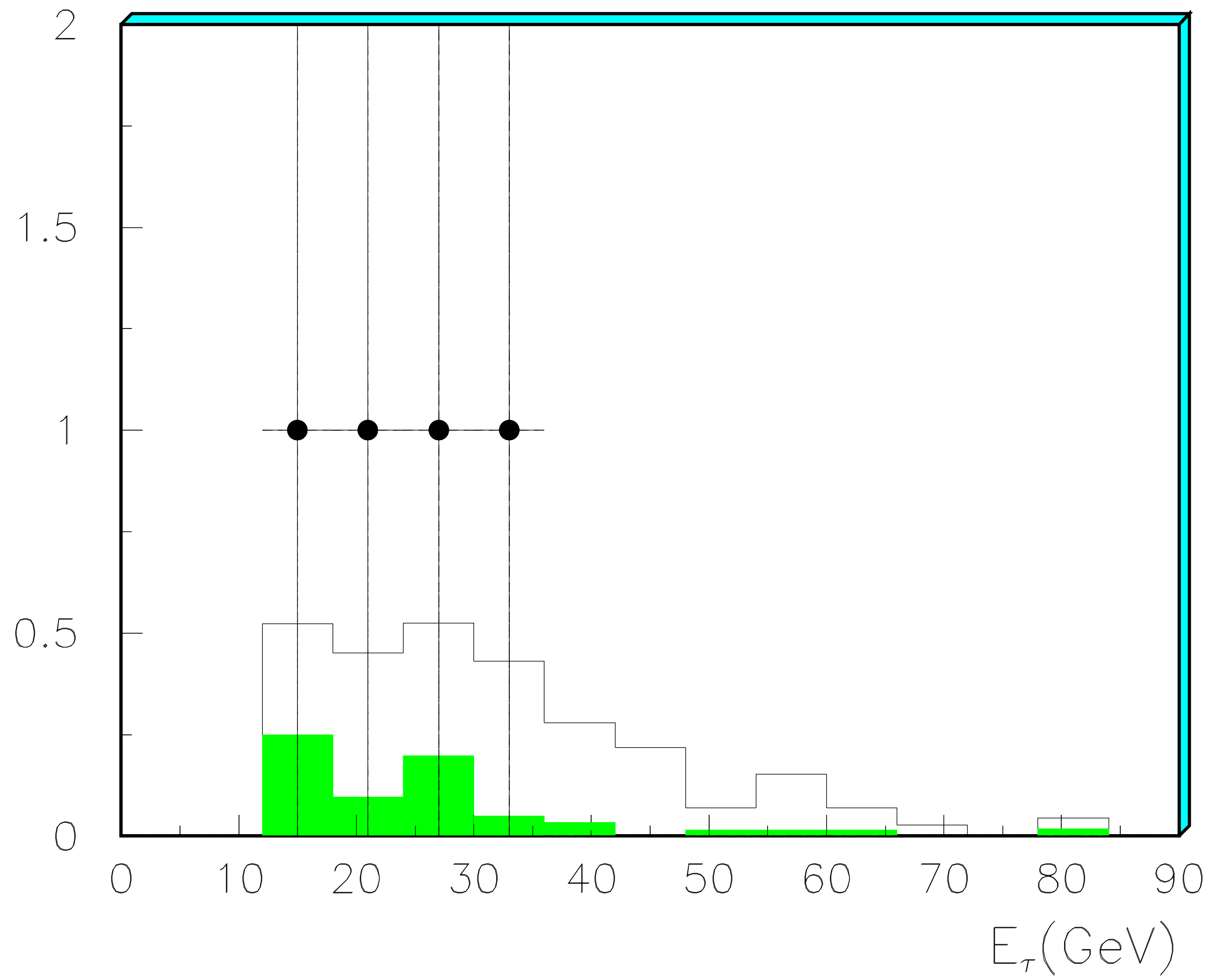

Figure 15: $W^- \to \tau^- \bar{\nu_\tau}$

Channel	Signal	BG	(Data)	Eff.(%)
$W^- \to \tau^- \bar{\nu_\tau}$	2.1	0.9	4	30.5

CERN

Events Selection

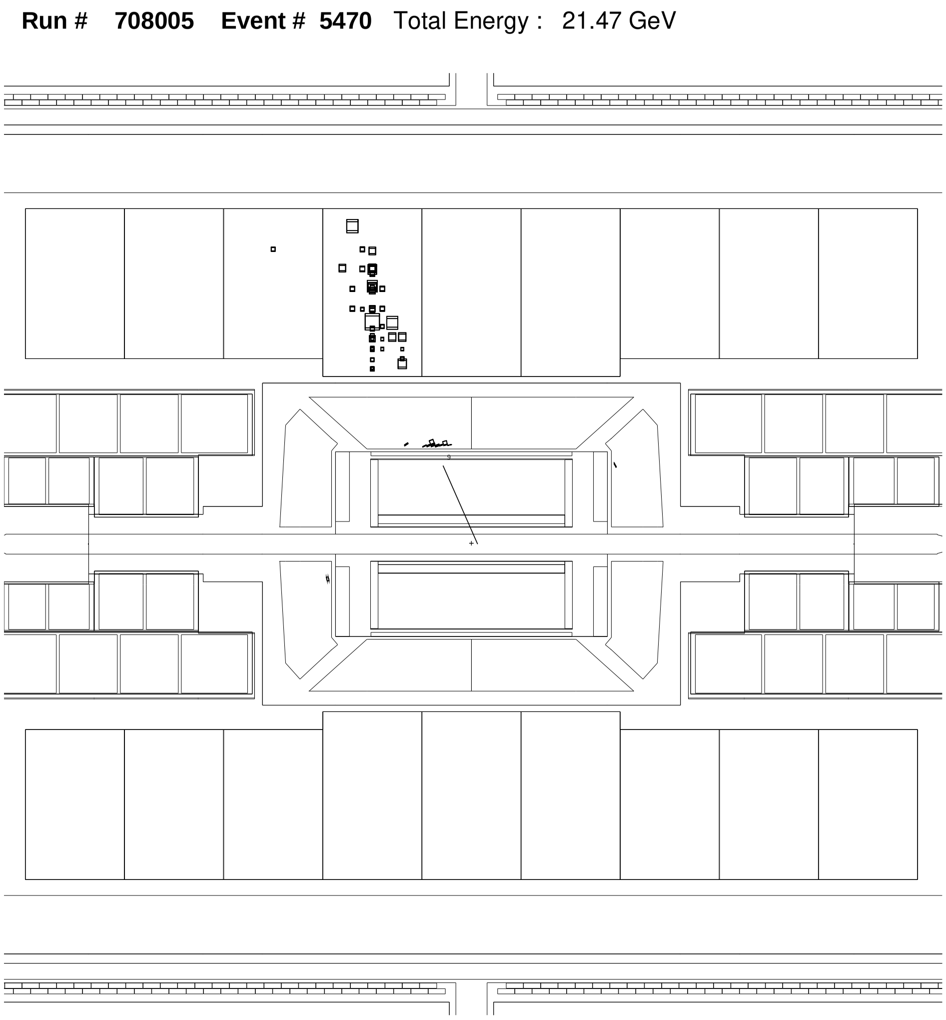

Figure 16: $W^- \to \tau^- \bar{\nu_\tau}$ candidate

$N_{trk} = 1,\ \theta_{sjt} = 69.5^\circ, E_{bgo} = 3.96\ GeV,$
$E_{hcal} = 17.1\ GeV,\ E_{sjt} = 21.1\ GeV.$

CERN

Events Selection

Selection cuts for $W^- \rightarrow q\bar{q}'$:

(1) $N_{trk} \geq 5, \quad N_{src} \geq 12$

(2) $50 < E_{tot} < 120\ GeV$

(3) $40 < M_{q\bar{q}'} < 120\ GeV$

(4) $Y_{23} < 0.1$

(5) $A_{cop} < 3.0\ Rad\ (172^\circ)$

(6) $|cos(\theta_{Thrust})| < 0.96\ (16^\circ)$

(7) $|cos(\theta_{mis})| < 0.95\ (18^\circ)$

(8) $E_{perp}/E_{tot} > 0.15$

(9) $E_{lumi} + E_{alr} < 65\ GeV$

Main Backgrounds after selection:
$W^+W^-,\ ZZ,\ q\bar{q},\ e^+e^-q\bar{q}, Ze^+e^-$.

CERN

Events Selection

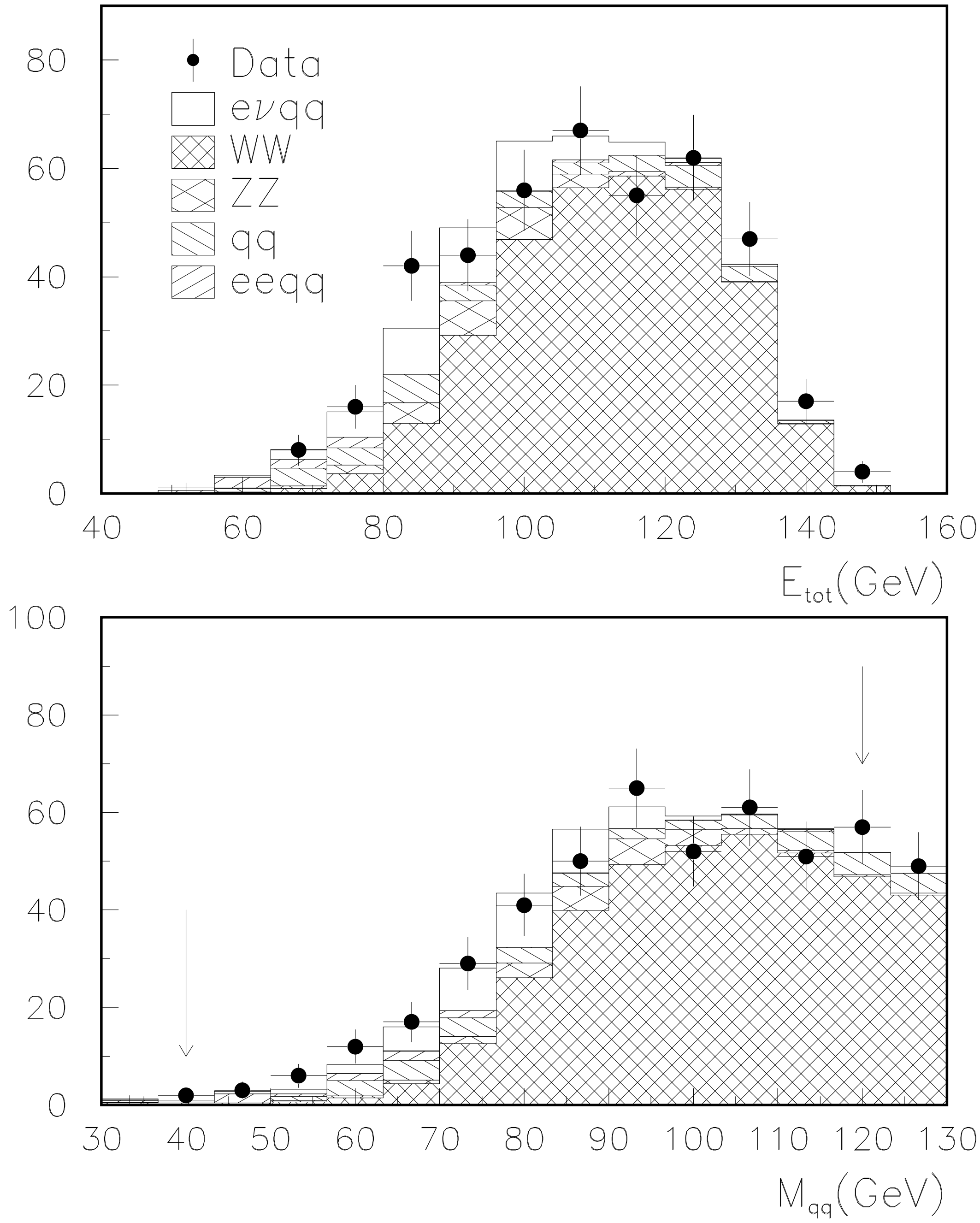

Figure 17: $W^- \to q\bar{q}'$

Events Selection

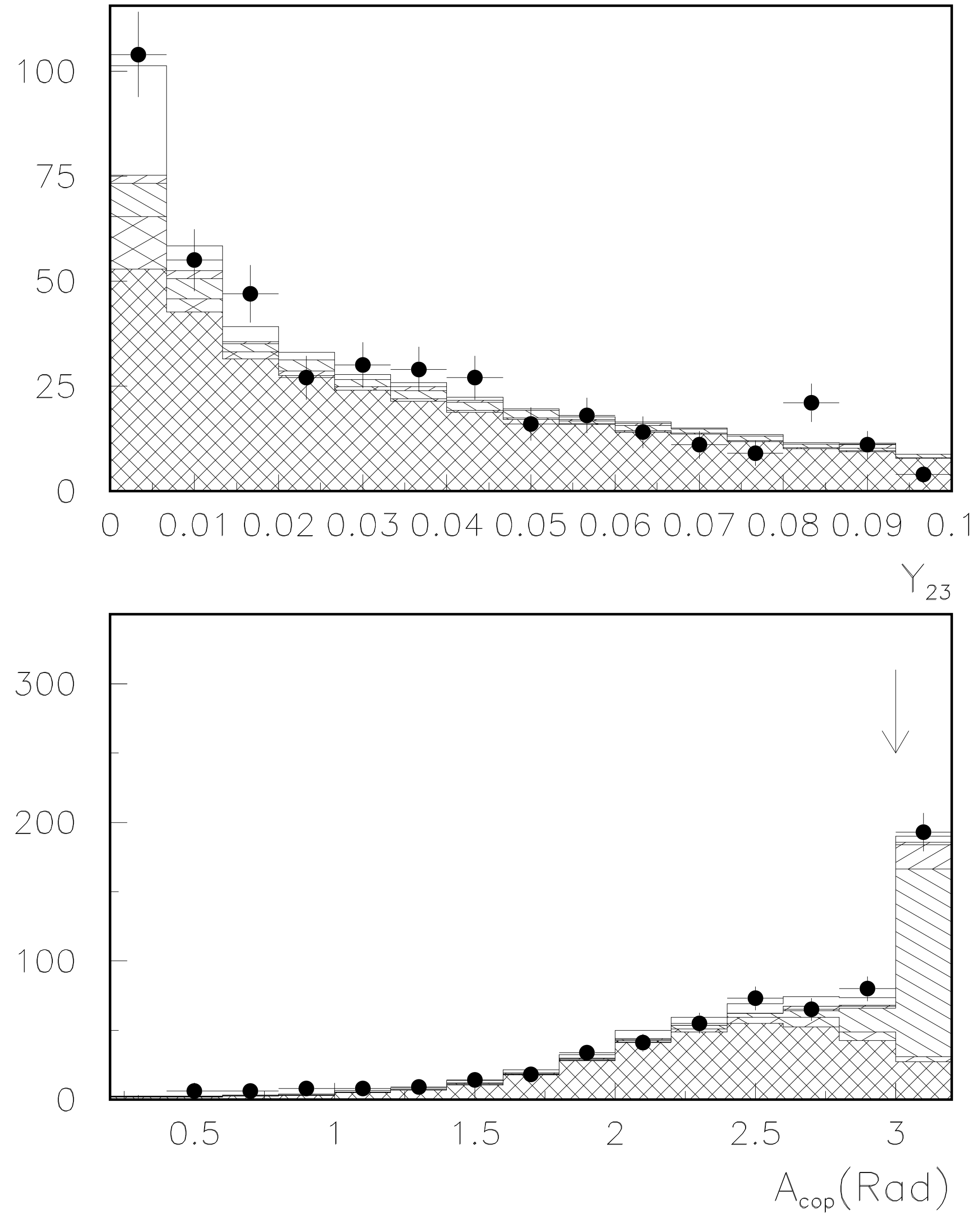

Figure 18: $W^- \to q\bar{q}'$

CERN

Events Selection

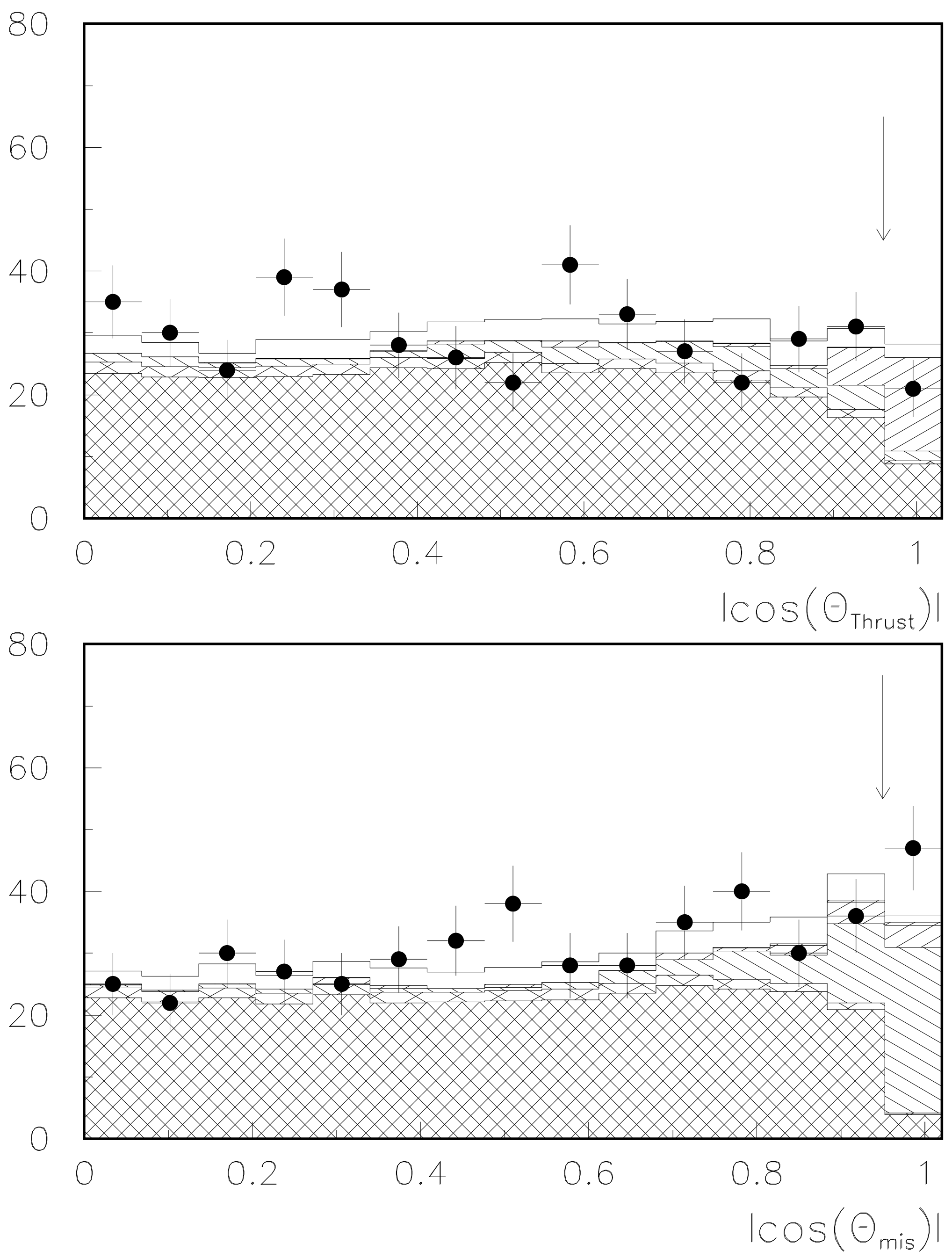

Figure 19: $W^- \to q\bar{q}'$

CERN

Events Selection

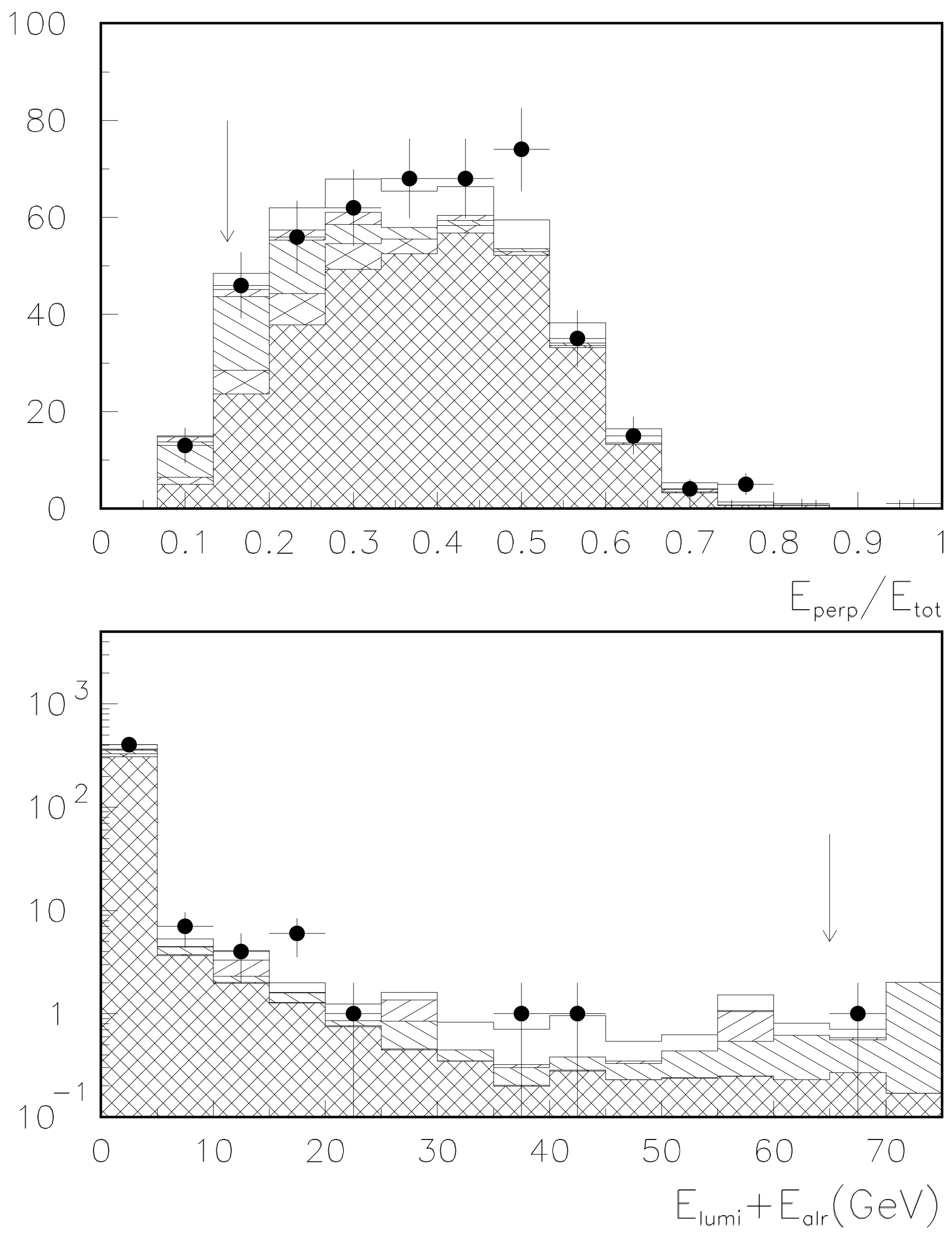

Figure 20: $W^- \to q\bar{q}'$

CERN

Events Selection

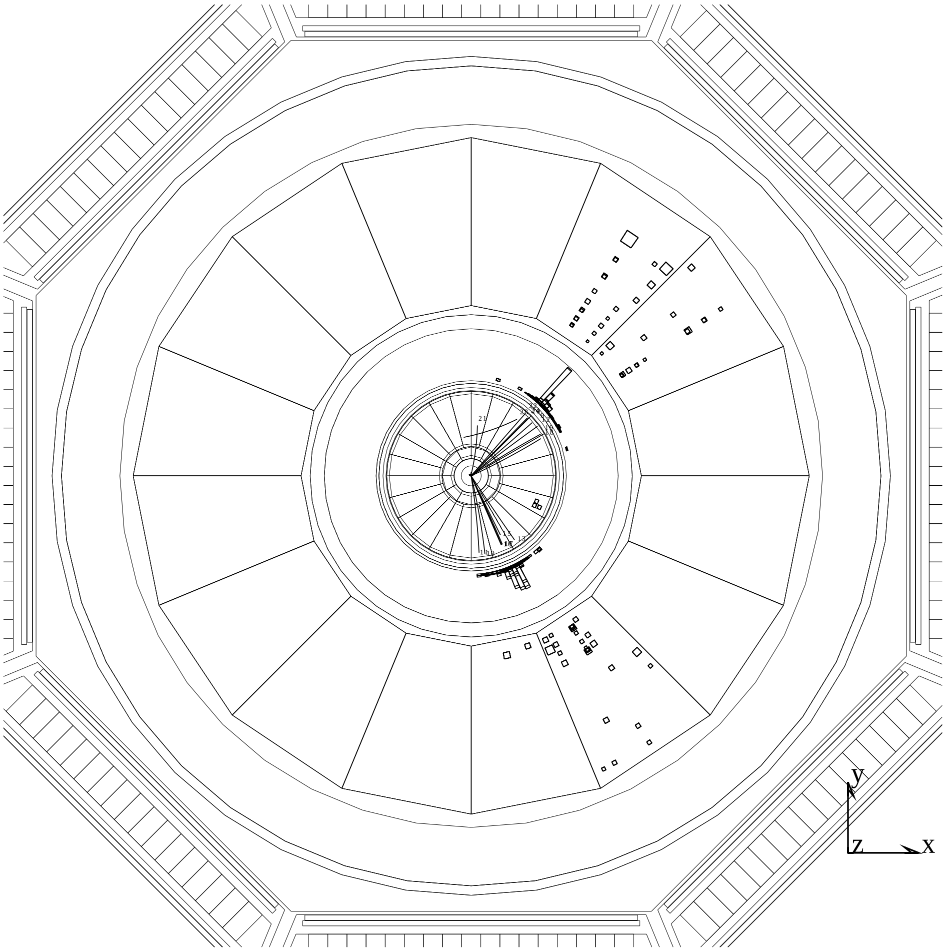

Figure 21: $W^- \rightarrow q\bar{q}'$ candidate

$N_{trk} = 15$, $M_{q\bar{q}'} = 80.4\ GeV$, $E_{perp}/E_{tot} = 0.53$,
$E_{bgo} = 82.8\ GeV$, $E_{hcal} = 11.9\ GeV$,
$A_{cop} = 1.9\ Rad$, $E_{tot} = 94.9\ GeV$.

Events Selection

Summary:

Table 3: Results of events selection.

Channels	Signal	BG	Data	Eff.(%)
$W^- \rightarrow e^- \bar{\nu}_e$	8.8	6.2	10	81.5
$W^- \rightarrow \mu^- \bar{\nu}_\mu$	6.7	4.0	13	51.1
$W^- \rightarrow \tau^- \bar{\nu}_\tau$	2.1	0.9	4	30.5
$W^- \rightarrow q\bar{q}'$	42.9	379.7	423	63.9

CERN

Measurement of Cross Section

Possion Distribution:

$$P(\kappa,\ \lambda) = \frac{\lambda^\kappa}{\kappa!} e^{-\lambda} \tag{8}$$

Binned Maximum Likelihood Fit:

$$\ln L = \ln \prod_i P(N^i_{obs},\ N^i_{exp})$$

$$= \sum_i \ln[\frac{(N^i_{exp})^{N^i_{obs}}}{N^i_{obs}\ !} e^{-N^i_{exp}}] \tag{9}$$

$$N^i_{exp} = \mathcal{L}(\sigma_s \varepsilon^i_s + \sigma_{bg} \varepsilon^i_{bg})$$

$$max(\ln L) \Longrightarrow \sigma_s$$

where

$\mathcal{L}$: *Total integrated luminosity*

N^i_{exp} : *MC expectation in i^{th} bin*

N^i_{obs} : *Observed events in i^{th} bin*

$\varepsilon^i_s,\ \varepsilon^i_{bg}$: *Eff. of Signal and BG in i^{th} bin*

$\sigma_s,\ \sigma_{bg}$: *Cross section of Signal and BG*

Measurement of Cross Section

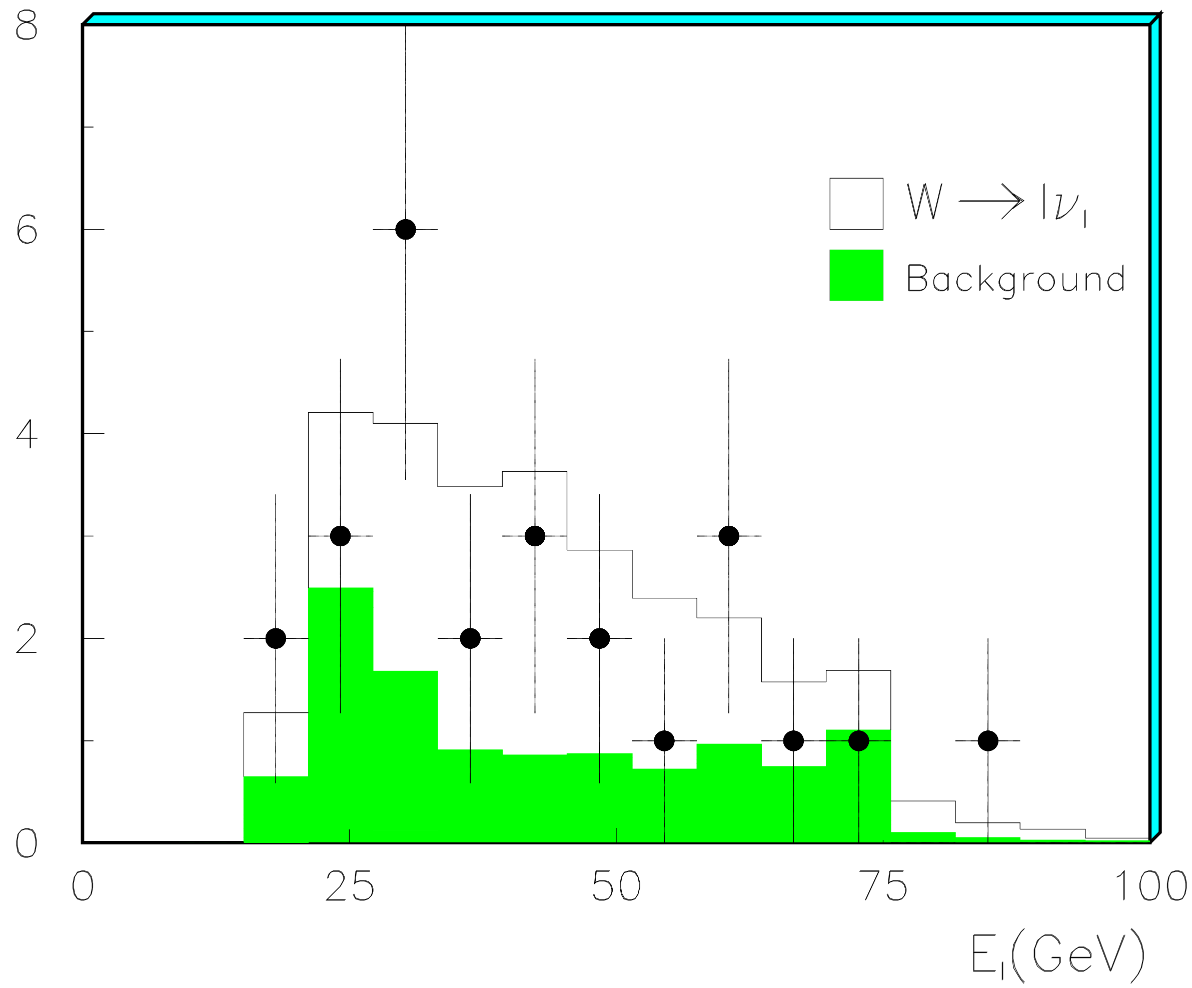

Figure 22: $W^- \rightarrow l^-\bar{\nu}_l$

$$\sigma_{W^-\rightarrow l^-\bar{\nu}_l} = 0.16^{+0.06}_{-0.05}\ pb$$

Measurement of Cross Section

Back-propagation Neural Network:

- 3 layers: input(8 nodes), hidden(8) and output(1)[0,1]
- Input parameters:

E_{tot}	E_{bgo}
E_{perp}/E_{tot}	E_{long}/E_{tot}
$M_{q\bar{q}'}$	Y_{23}
A_{cop}	P_{mis}

- Supervised training:

  Signal: $W^- \rightarrow q\bar{q}'(520)$,
  Noise: $WW(29000)$,
  Traing Loop: 1000000,
  Temperature T $= 1.0$,
  Momentum $\beta = 0.07$,
  Training Rate $\alpha = 0.03 \rightarrow 0.005$.

CERN

Measurement of Cross Section

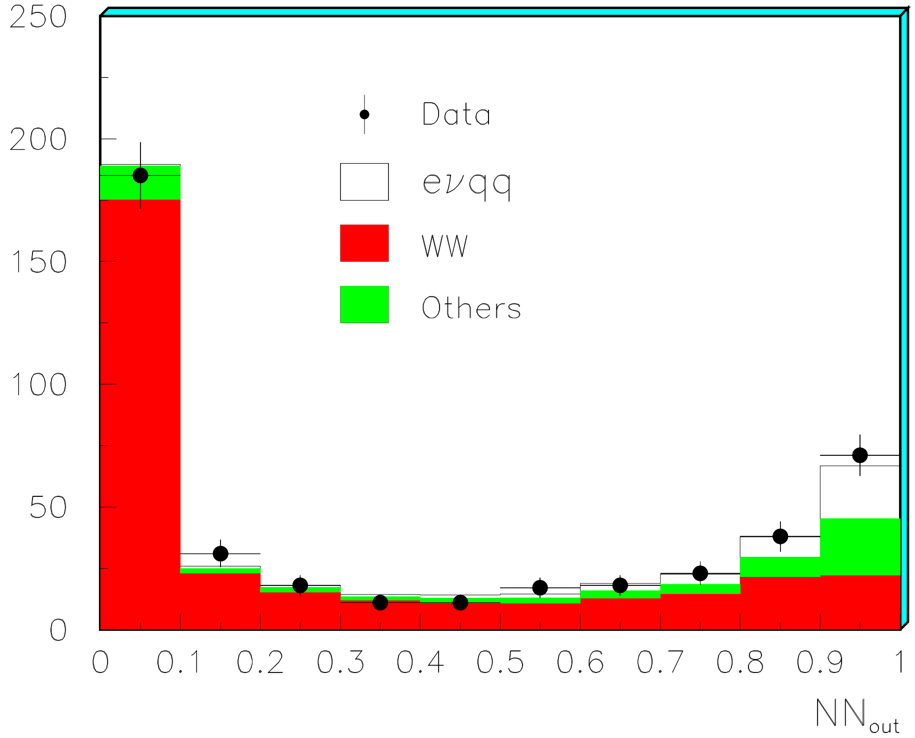

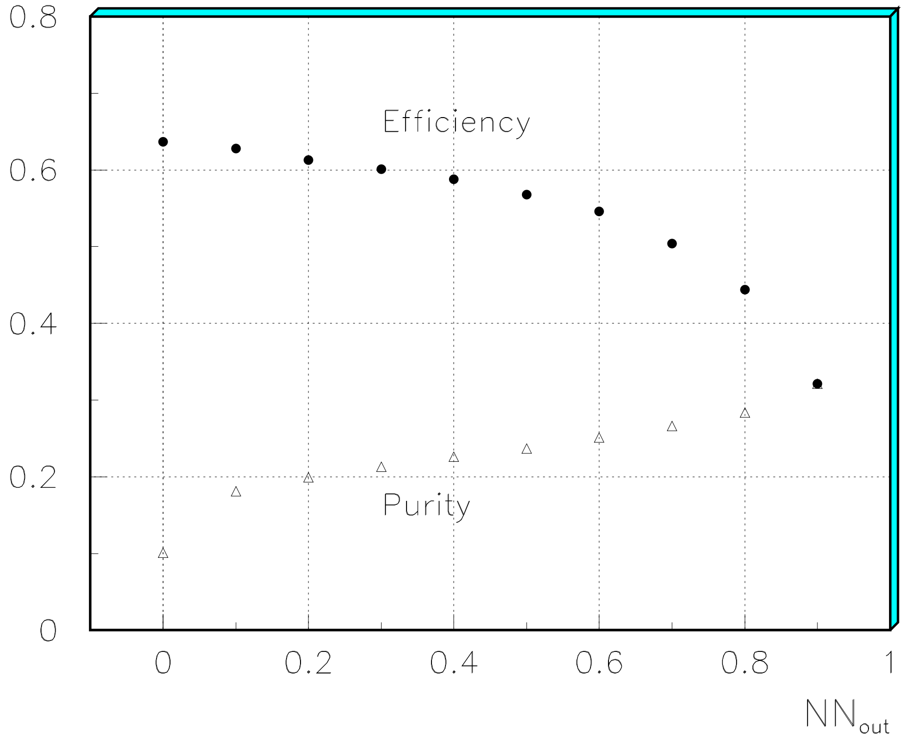

CERN

Measurement of Cross Section

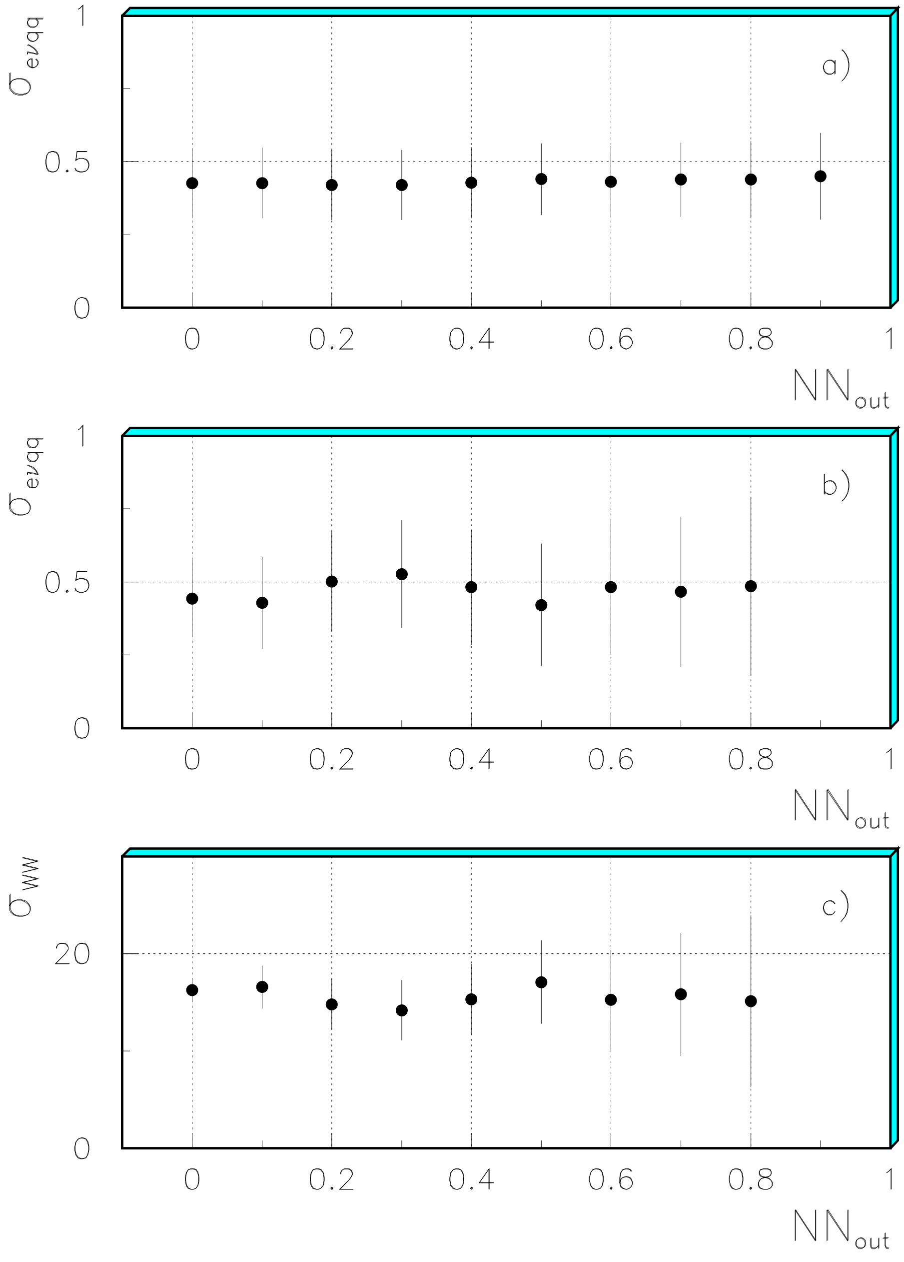

Figure 23: σ_s and σ_{WW} as a function of NN_{out}.

CERN

Measurement of Cross Section

- 1-parameter fit:

  $\sigma_{W^- \to q\bar{q}'} = 0.42 \pm 0.12 \ pb$

- 2-parameter fit:

  $\sigma_{W^- \to q\bar{q}'} = 0.44 \pm 0.13 \ pb$

  $\sigma_{W^+W^-} = 16.3 \pm 1.1 \ pb$ (for cross check)

  $\sigma_{W^+W^-} = 16.2 \pm 0.37 \pm 0.27 \ pb$ (L3 Result).

Summary:

Channels	σ(pb)	stat. error	syst. error
$W^- \to l^- \bar{\nu}_l$	0.16	${}^{+0.06}_{-0.05}$	± 0.02
$W^- \to q\bar{q}'$	0.42	± 0.12	± 0.03
Total	0.58	± 0.13	± 0.04
L3 Result	0.53	${}^{+0.12}_{-0.11}$	± 0.03

CERN

Measurement of Cross Section

Table 4: Evaluation of Systematic Error.

(Sources)	$W^- \to l^- \bar{\nu}_l$ (pb)	$W^- \to q\bar{q}'$ (pb)
MC Statistics	0.014	0.005
Selection Cuts	0.015	0.010
Uncertainty on σ_{bg}	0.004	0.015
Network Stability	–	0.010
EXCALIBUR & GRC4F	0.005	0.016
Total	0.022	0.027

Measurement of Cross Section

Cross sections of Single W at LEP2.

$\sqrt{s}$ (GeV)	$\sigma_{e^+\nu_e W^-}$ (pb)
161	$0.46^{+0.47}_{-0.35} \pm 0.04$
172	$0.60^{+0.59}_{-0.44} \pm 0.04$
183	$0.62^{+0.22}_{-0.19} \pm 0.04$
189	$0.53^{+0.12}_{-0.11} \pm 0.03$
189(this analysis)	$0.58^{+0.13}_{-0.13} \pm 0.04$

Table 5: $\sigma_{W^-e^+\nu_e}$ measured by L3 in different Centre-of-Mass Energy (68%C.L.).

All measured cross sections are consistent with Standard Model predictions.
SM predictions at 189 GeV are:

EXCALIBUR: 0.57 pb,

GRC4F: 0.56 pb.

CERN

Measurement of Cross Section

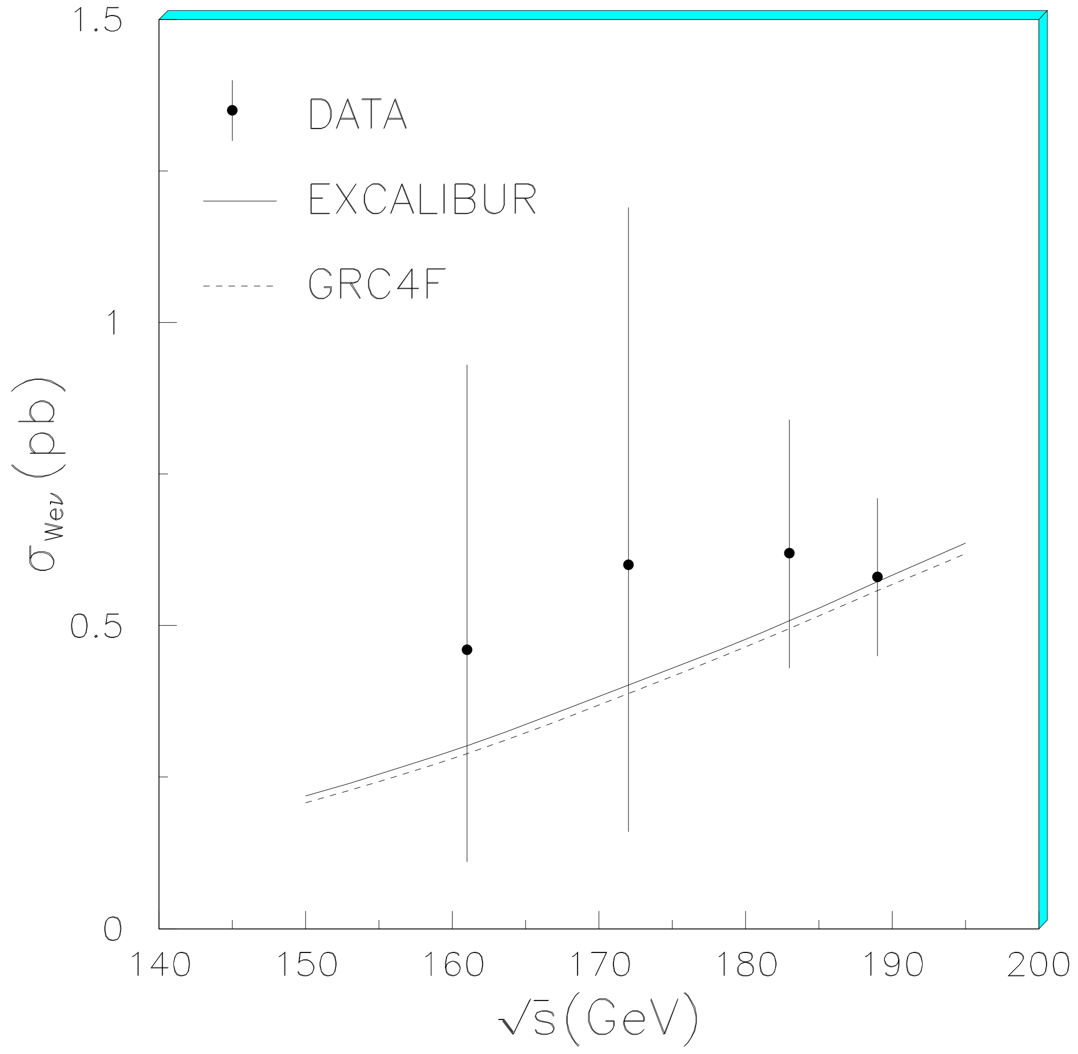

Figure 24: The cross sections of Single W ($\sigma_{We\nu_e}$) as a function of Center-of-Mass Energy.

CERN

Anomalous Couplings Fit

- Differential Cross Section:

$$d\sigma(\Delta\kappa_\gamma,\ \lambda_\gamma) = a_0 + a_1\Delta\kappa_\gamma + a_2\Delta\kappa_\gamma{}^2 + a_3\Delta\kappa_\gamma\lambda_\gamma + a_4\lambda_\gamma + a_5\lambda_\gamma{}^2 \tag{10}$$

- In order to normalize a_0, we define event **Weight** R_i:

$$R_i(4M,\ \Psi_{fit}) = \frac{d\sigma_i(\Psi_{fit})}{d\sigma_i(\Psi_{gen})} = \frac{|M_i(4M,\ \Psi_{fit})|^2}{|M_i(4M,\ \Psi_{gen})|^2} \tag{11}$$

- So, total cross section of signal becomes:

$$\sigma(\Psi_{fit}) = \frac{\sigma_{gen}}{N_{gen}} \bullet \sum_i^{N_{gen}} R_i(\Psi_{fit}) = \sigma_{gen} \bullet R(\Psi_{fit}) \tag{12}$$

$$R(\Psi_{fit}) = 1.0 + a_1\Delta\kappa_\gamma + a_2\Delta\kappa_\gamma{}^2 + a_3\Delta\kappa_\gamma\lambda_\gamma + a_4\lambda_\gamma + a_5\lambda_\gamma{}^2$$

Anomalous Couplings Fit

Binned Maximum Likelihood Fit:

$$\ln L = \ln \prod_i P(N^i_{obs},\ N^i_{exp}) = \sum_i \ln\left[\frac{(N^i_{exp})^{N^i_{obs}}}{N^i_{obs}\ !} e^{-N^i_{exp}}\right] \tag{13}$$

where

$$\begin{aligned} N^i_{exp} &= \mathcal{L}(\sigma_s \varepsilon^i_s + \sigma_{bg1}\varepsilon^i_{bg1} + \sigma_{bg2}\varepsilon^i_{bg2}) \\ &= \mathcal{L}[\sigma^{gen}_s R_s(\Psi_{fit})\varepsilon^i_s + \sigma^{gen}_{bg1} R_{bg1}(\Psi_{fit})\varepsilon^i_{bg1} + \sigma_{bg2}\varepsilon^i_{bg2}] \\ max &\quad (\ln L) \Longrightarrow \Psi_{fit} = (\Delta\kappa_\gamma,\ \lambda_\gamma) \end{aligned}$$

bg1: sensitive to anomalous couplings,

bg2: insensitive to anomalous couplings.

CERN

Anomalous Couplings Fit

Measurement of Coefficiencies:

$R(\Delta\kappa_\gamma,\ \lambda_\gamma)$	$\Delta\kappa_\gamma$	λ_γ
$R(0,\ 0)$	0	0
$R(-1,\ 0)$	-1	0
$R(1,\ 0)$	1	0
$R(0,\ -1)$	0	-1
$R(0,\ 1)$	0	1
$R(1,\ 1)$	1	1

$$\left(\begin{array}{rcl} a_1 &=& [R(1,\ 0) - R(-1,\ 0)]/2.0 \\ a_2 &=& [R(1,\ 0) + R(-1,\ 0)]/2.0 - 1.0 \\ a_3 &=& R(1,\ 1) - (1.0 + a_1 + a_2 + a_4 + a_5) \\ a_4 &=& [R(0,\ 1) - R(0,\ -1)]/2.0 \\ a_5 &=& [R(0,\ 1) + R(0,\ -1)]/2.0 - 1.0 \end{array}\right) \tag{14}$$

CERN

Anomalous Couplings Fit

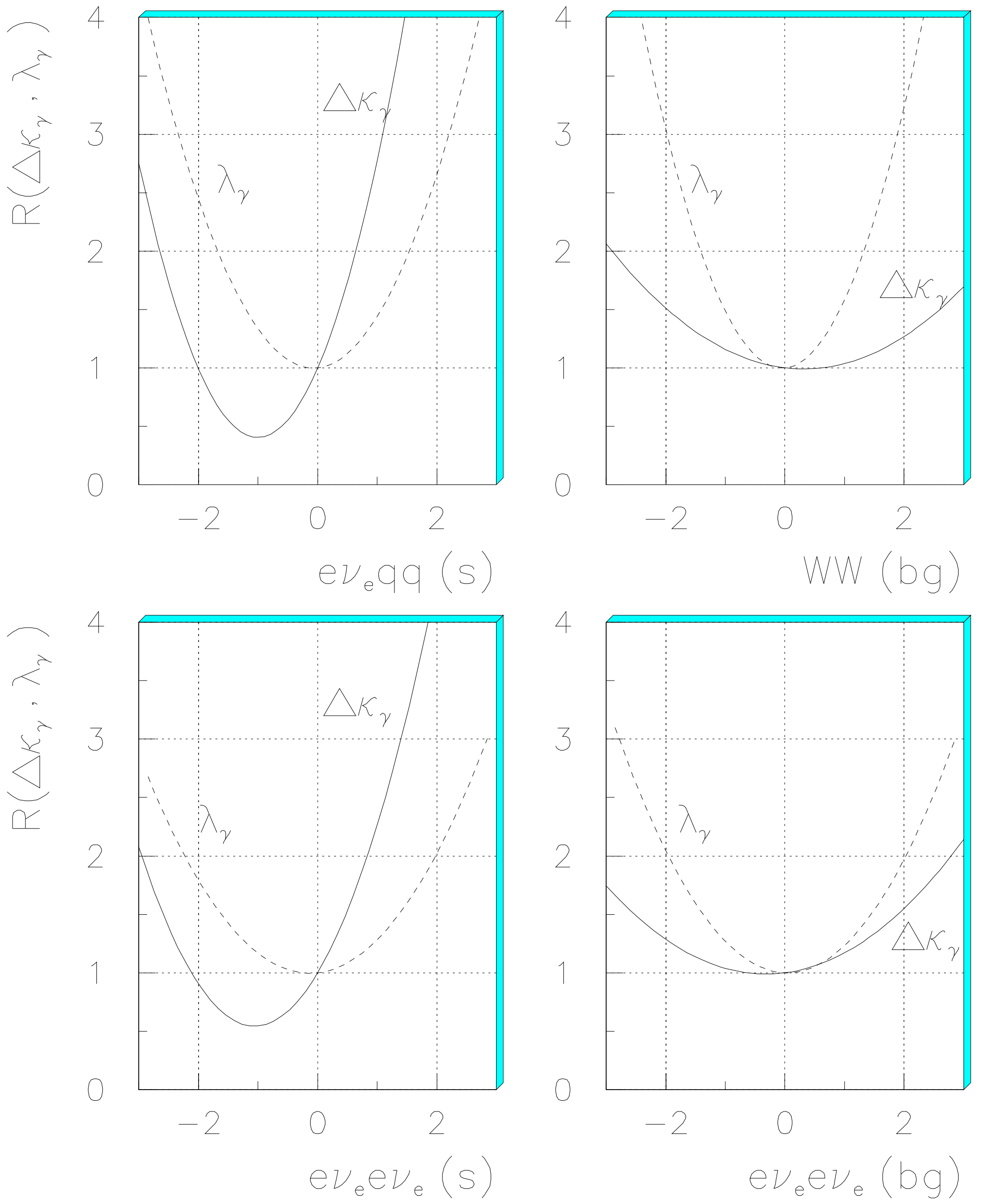

Figure 25: Weights of $e^+\nu_e q\bar{q}'$, W^+W^-, $e^+\nu_e e^-\bar{\nu_e}(s,bg)$ as a function of $\Delta\kappa_\gamma$ and λ_γ.

CERN

Anomalous Couplings Fit

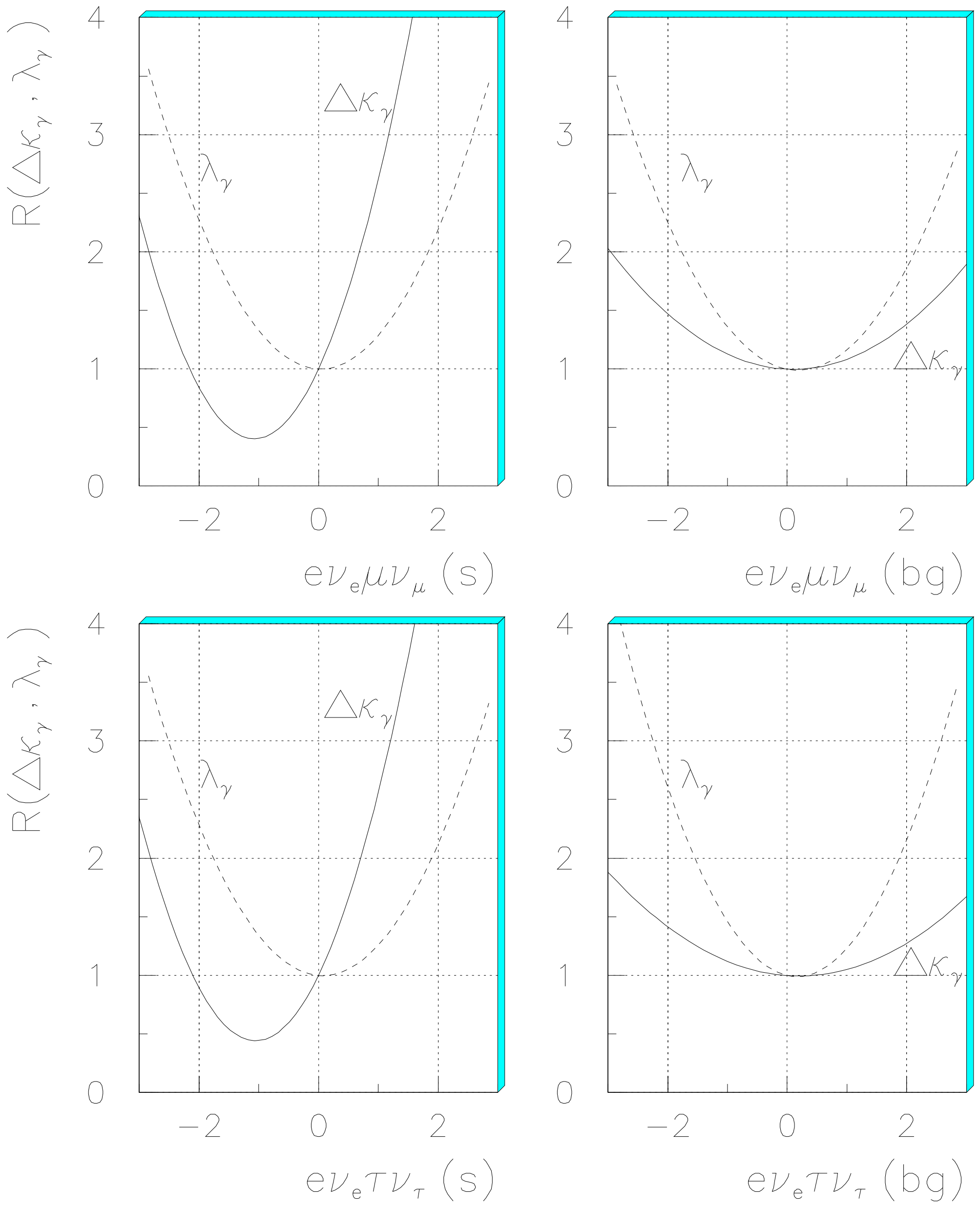

Figure 26: Weights of $e^+\nu_e\mu^-\bar{\nu_\mu}, e^+\nu_e\tau\bar{\nu_\tau}(s, bg)$ as a function of $\Delta\kappa_\gamma$ and λ_γ.

CERN

Anomalous Couplings Fit

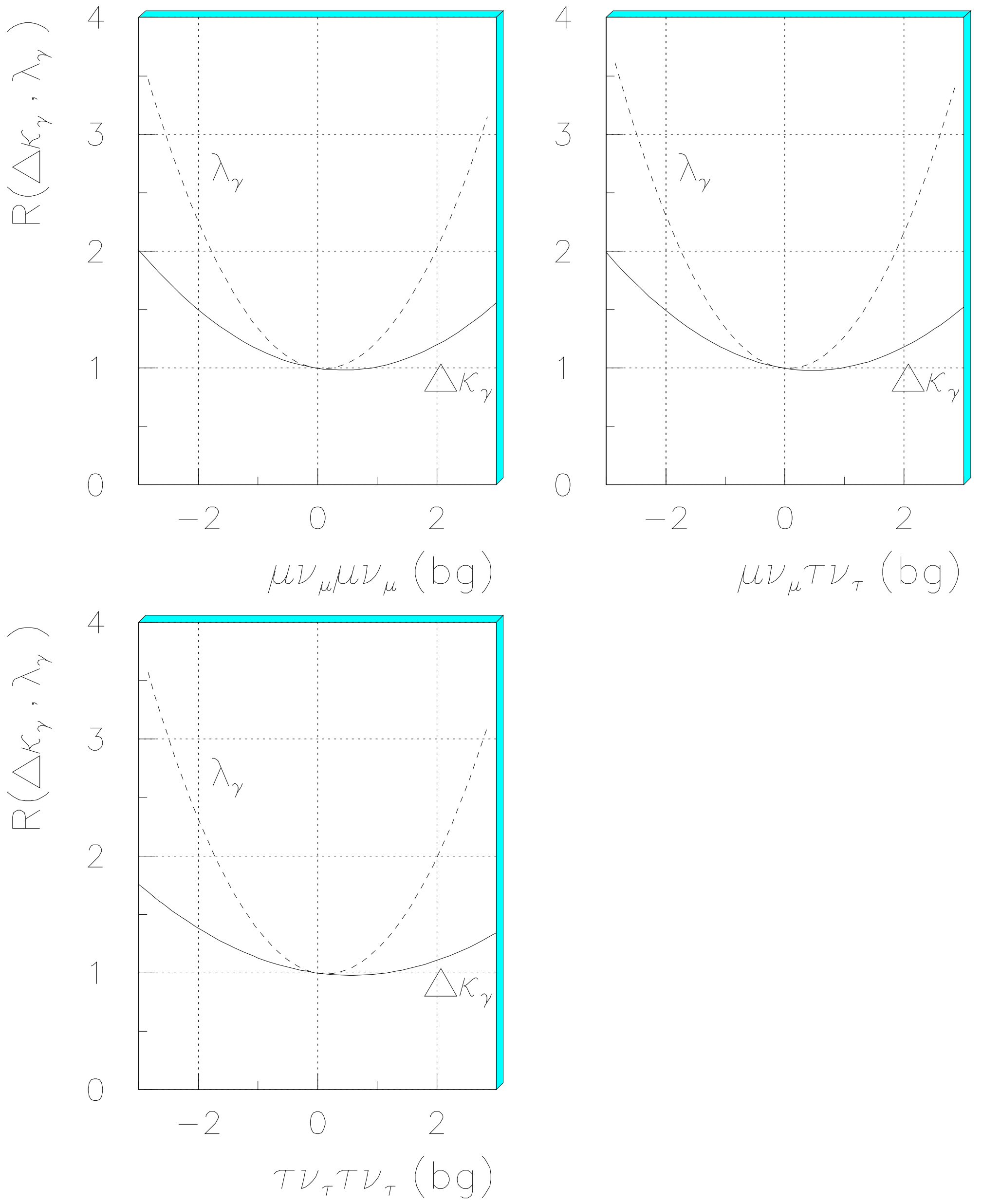

Figure 27: Weights of $\mu^+\nu_\mu\mu^-\bar{\nu_\mu}$, $\mu^+\nu_\mu\tau^-\bar{\nu_\tau}$, $\tau^+\nu_\tau\tau^-\bar{\nu_\tau}(bg)$ as a function of $\Delta\kappa_\gamma$ and λ_γ.

CERN

Anomalous Couplings Fit

Measurement of $\Delta\kappa_\gamma$ and λ_γ:

(1). Single W contribution, fix WW.

	C.L.	$\Delta\kappa_\gamma$	λ_γ
1-P	68%	$0.01\ ^{+0.19}_{-0.22}$ [- 0.21, 0.20]	$-0.34\ ^{+1.06}_{-0.52}$ [- 0.86, 0.72]
	95%	$0.01\ ^{+0.35}_{-0.47}$ [- 0.46, 0.36]	$-0.34\ ^{+1.41}_{-0.84}$ [- 1.18, 1.07]
2-P	68%	$-0.20\ ^{+0.39}_{-1.99}$ [- 2.19, 0.19]	$-0.81\ ^{+2.13}_{-0.72}$ [- 1.53, 1.32]
	95%	$-0.20\ ^{+0.56}_{-2.17}$ [- 2.37, 0.36]	$-0.81\ ^{+2.36}_{-0.95}$ [- 1.76, 1.55]

Anomalous Couplings Fit

(2). Single W + WW contribution.

	C.L.	$\Delta\kappa_\gamma$	λ_γ
1-P	68%	$0.02\ ^{+0.19}_{-0.22}$ [- 0.20, 0.21]	$-0.10\ ^{+0.37}_{-0.27}$ [- 0.37, 0.27]
	95%	$0.02\ ^{+0.36}_{-0.50}$ [- 0.48, 0.38]	$-0.10\ ^{+0.51}_{-0.40}$ [- 0.50, 0.41]
2-P	68%	$0.01\ ^{+0.19}_{-0.23}$ [- 0.22, 0.20]	$-0.10\ ^{+0.37}_{-0.28}$ [- 0.38, 0.27]
	95%	$0.01\ ^{+0.36}_{-0.49}$ [- 0.48, 0.37]	$-0.10\ ^{+0.51}_{-0.41}$ [- 0.51, 0.41]

CERN

Anomalous Couplings Fit

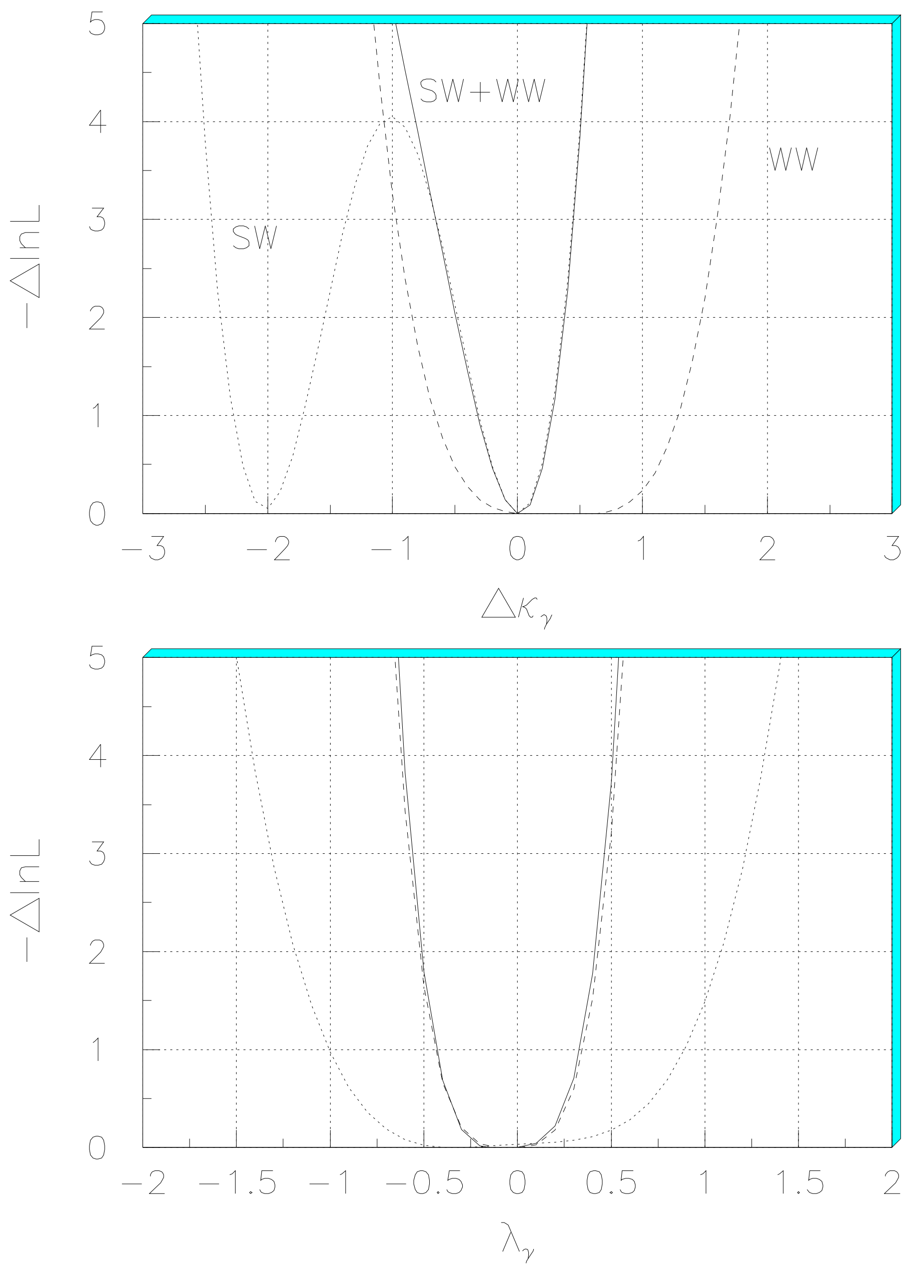

Figure 28: $-\Delta \ln L$ as a function of $\Delta\kappa_\gamma$ and λ_γ.

CERN

Anomalous Couplings Fit

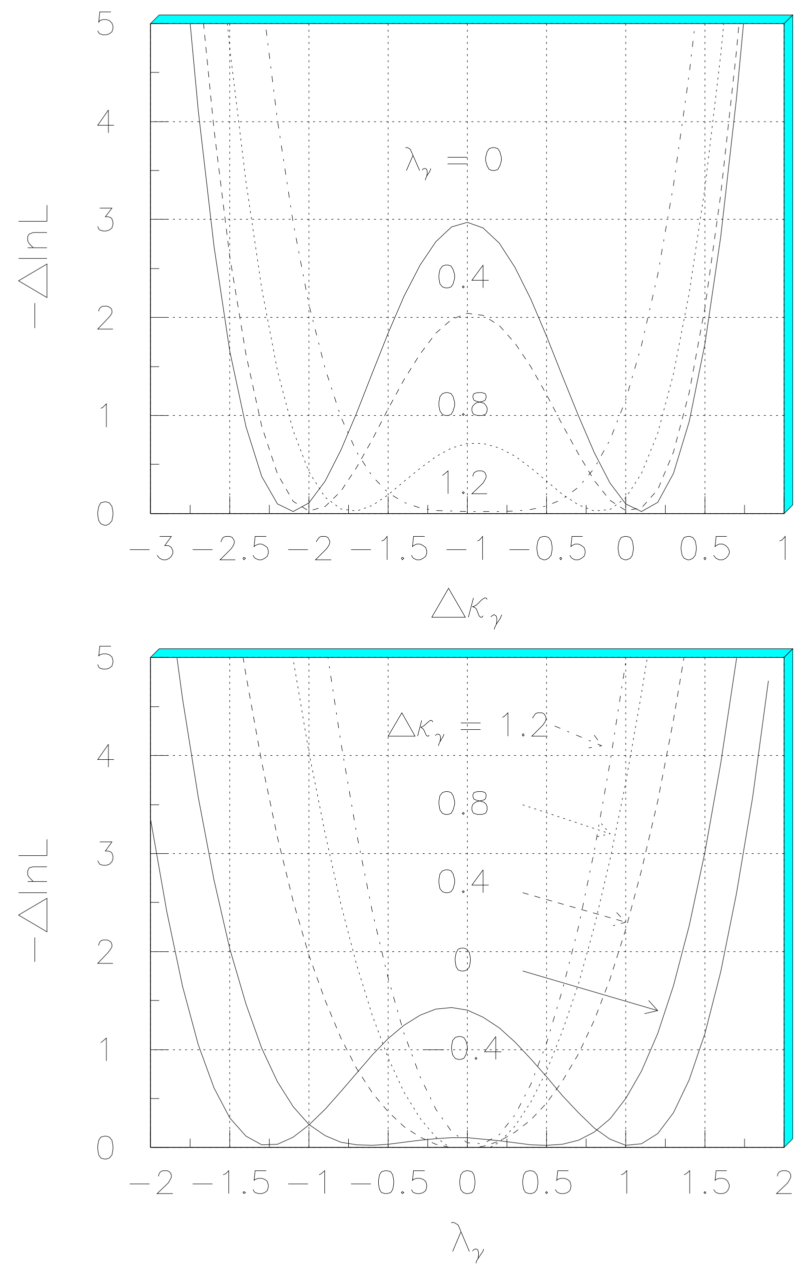

Figure 29: Single W (h) contribution only.

Anomalous Couplings Fit

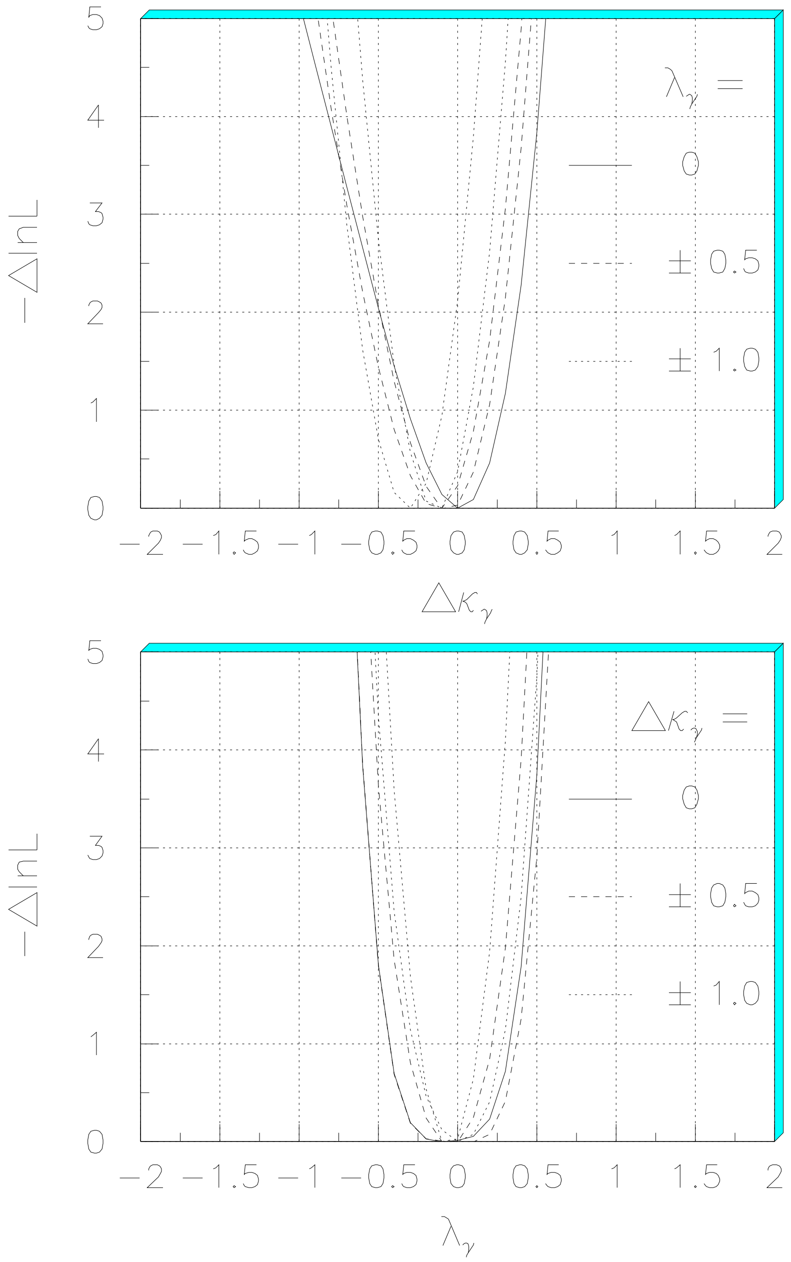

Figure 30: Single W + WW contributions.

Anomalous Couplings Fit

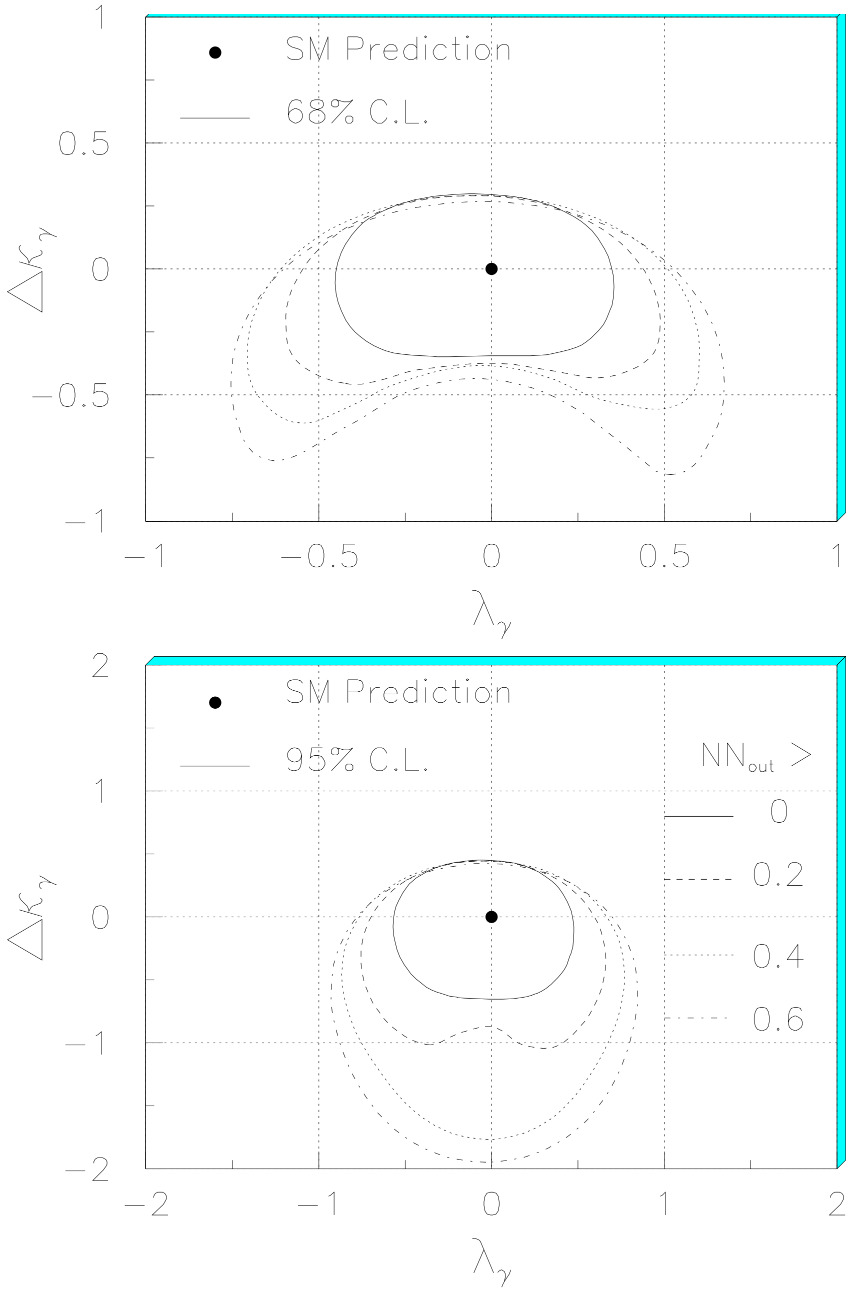

Figure 31: Contours of $\Delta\kappa_\gamma - \lambda_\gamma$ corresponding to 68% and 95% C.L. for different NN_{out}.

CERN

Anomalous Couplings Fit

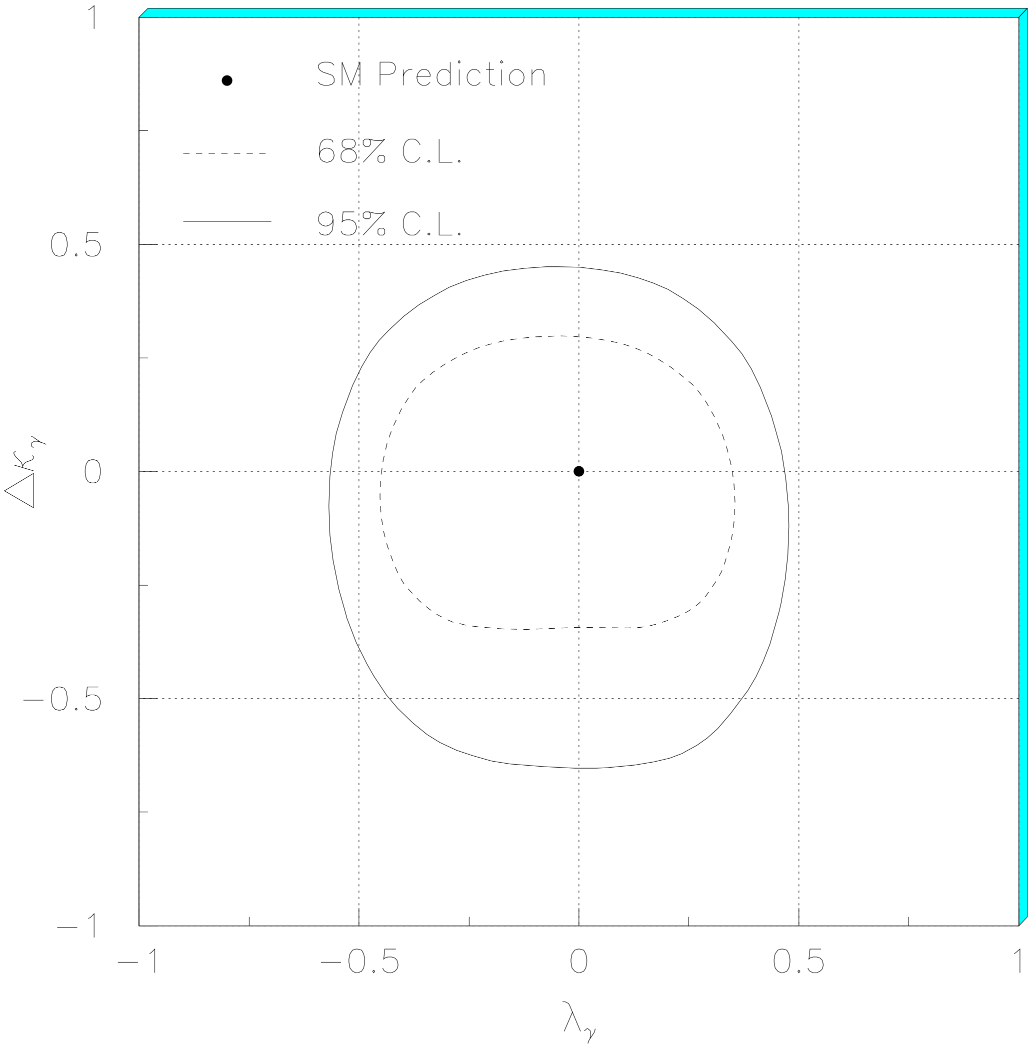

Figure 32: Contours of $\Delta\kappa_\gamma - \lambda_\gamma$.

CERN

Anomalous Couplings Fit

Table 6: Compare with other results, 95% C.L..

	$\sqrt{s}(GeV)$	$\mathcal{L}(pb^{-1})$	$\Delta\kappa_\gamma$	λ_γ
L3 SW(2-p)	130-183	88.5	[- 0.46, 0.57]	[- 0.86, 0.75]
L3 SW(2-p)	130-189	264.9	[- 0.42, 0.22]	[- 0.64, 0.61]
L3 WW(2-p)	161-189	253	[- 0.41, 0.24]	[- 0.12, 0.18]
this analysis				
SW+WW(2-p)	189	176.4	[- 0.48, 0.37]	[- 0.51, 0.41]
SW(1-p)	189	176.4	[- 0.46, 0.36]	[- 1.18, 1.07]

CERN

Conclusions

Single W Production at 189 GeV

- Cross section is measured to be:

  $\sigma_{W^- e^+ \nu_e} = 0.58 \pm 0.13(stat.) \pm 0.04(syst.)\ pb$

- Limits on $WW\gamma$ couplings at 95% C.L.

  Single W contribution:

  $$-0.46 < |\Delta\kappa_\gamma| < 0.36\ (\lambda_\gamma = 0)$$

  $$-1.18 < |\lambda_\gamma| < 1.07\ (\Delta\kappa_\gamma = 0)$$

  Single W and WW contributions:

  $$-0.48 < |\Delta\kappa_\gamma| < 0.38\ (\lambda_\gamma = 0)$$

  $$-0.50 < |\lambda_\gamma| < 0.41\ (\Delta\kappa_\gamma = 0)$$

- $\Delta\kappa_\gamma$ is comparable to that from WW.

CERN

Acknowledgements

The work described in the presentation is the result of a combined effort of many people. I would like to mention some of them in particular.

Special thanks go to my supervisors Prof. Tang Xiaowei, Dr. Martin Pohl and Dr. Guoming Chen for their guidance and constructive suggestions.

I thank Prof. H.Hofer and M.Jongmanns from ETH,Zurich for their financial support.

Thanks to Prof. H.S.Chen, Y.S.Lu, G.L.Tong, B.N.Jin and H.L Zhuang for their care and support.

Many thanks to colleagues working in WW group for their help and suggestions on the subject. The work can't run smoothly without their help.

I thank Dr. M.Yang and Z.H.Xiong for the introduction and helpful discussion on the topic at very first time. I acknowledge Dr. C.G.Yang, G.Chen, Z.A.Liu, H.T.Liu, L.Lu, G.Y.Zhu and other colleagues for their kindly help.

Last but not least, thank my parents and my lover for their infinite love and support.

CERN